AMNIOTIC MEMBRANE AS A SCAFFOLD FOR HUMAN ADIPOSE STEM CELLS AND UMBILICAL VEIN ENDOTHELIAL CELLS

Mia Zhou

Syventävien opintojen kirjallinen työ

Tampereen yliopisto

Lääketieteen ja biotieteiden tiedekunta

Joulukuu 2017

Tampereen yliopisto

Lääketieteen ja biotieteiden tiedekunta

Adult stem cell group, Biomeditech, Tampereen yliopisto

ZHOU MIA: AMNIOTIC MEMBRANE AS A SCAFFOLD FOR HUMAN ADIPOSE STEM CELLS AND UMBILICAL VEIN ENDOTHELIAL CELLS

Kirjallinen työ, 42 s. Ohjaaja: dosentti Susanna Miettinen, Biomeditech, Tampereen yliopisto

Joulukuu 2017

Avainsanat: tissue engineering, amniotic membrane, adult stem cells, adipose-derived stem cells, human umbilical vein endothelial cells, angiogenesis

The amniotic membrane (AM) has many desirable qualities for tissue engineering. The three main objectives of this study were to investigate 1) adipose-derived stem cell (ASC) cultivation and possible differentiation on AM, 2) co-cultivation of ASCs and human umbilical vein endothelial cells (HUVECs) on AM for enhanced angiogenesis, 3) effects of cell cultivation on the mechanical properties of AM.

Denuded AM was cut and placed to cover the bottom of 6-well multidishes, 1/3 of AM-covered wells were seeded with only ASCs, 1/3 with only HUVECs and 1/3 with both. Half were cultured with adipose medium (ADM) and half with endothelial medium for three weeks (EM).

After three weeks, the cultivated AMs were analyzed with quantitative real-time polymerase chain reaction (RT-PCR), immunofluorescence photography, hematoxylin-eosin staining and microtomography. Tensile strength tests were conducted with separate AM samples cultivated in special scaffolds along with nitrocellulose paper.

Results showed no visible adipose formation, nor clear angiogenic tube formation. Engineering stress endured by AM during tension testing decreased as cultivation time lengthened. ASCs showed great viability on AM. HUVECs showed viability in EM based on von Willebrand factor expression. HUVEC proliferation was not seen in ADM. In conclusion, AM is a suitable scaffold for ASCs, better induction agents for adipocyte differentiation and tube formation should be explored, and a better method to detect HUVECs from the co-cultivation wells is needed.

1. Introduction

1.1.Tissue engineering

Tissue engineering and regenerative medicine rose to prominence in the late 1980s as other treatment options for organ failure and tissue loss proved less efficient and more problematic than imagined. The queue for organ transplantation was long and allogeneic transplantation caused immunological rejection in some recipients. Artificial materials and mechanical devices i.e. artificial joints, dialysis machine, were too simple to replace all functions of a human organ (1).

The basis of tissue engineering is the production of new tissue through cultivation of isolated cells in tissue-inducing substances e.g. growth factors in matrix or on scaffolding (Figure **1**) (1).

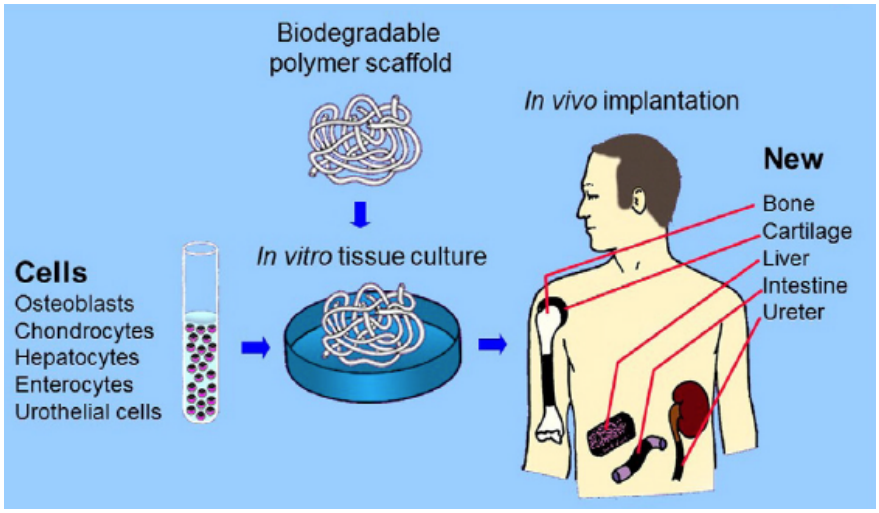

Figure 1 - Principles of tissue engineering (2)

Virtually every tissue and organ of the human body has been the subject for tissue engineering e.g. bone, cartilage, muscle, skin and spinal cord to name a few (2). Stem cells have always been a subject of interest in tissue engineering since they can differentiate into multiple cell lines, thus can be tailored individually for each application (3).

Different matrix materials have been tested, from synthetic materials such as lactic-glycolic acid or polyacrylonitrile-polyvinyl chloride to natural materials like collagen or hydroxyapatite. The mechanical properties of synthetic materials are easier to control; natural materials on the other hand mimic in-vivo

extracellular matrix in which the cultivated cells can be naturally found. (3) In this study, the suitability of amniotic membrane (AM) as a tissue engineering scaffold will be examined.

1.2.Amniotic membrane

The amniotic membrane is one of the two fetal membranes, the other being the chorion. The membranes are formed during early embryo development, around the 8^{th} -9^{th} day of gestation. AM lines the amniotic cavity, which is full of amniotic fluid. The amniotic fluid is partly produced by the cells of the AM, but mostly it is derived from maternal blood. The embryo and later on fetus, is immersed in the fluid, which absorbs jolts and allows fetal movement inside the mother. The amniotic cavity lies within the chorionic cavity, as the amnion grows, it fills the chorionic cavity completely. Even though AM covers the chorion from the inside, the two membranes stay separated instead of fusing (4).

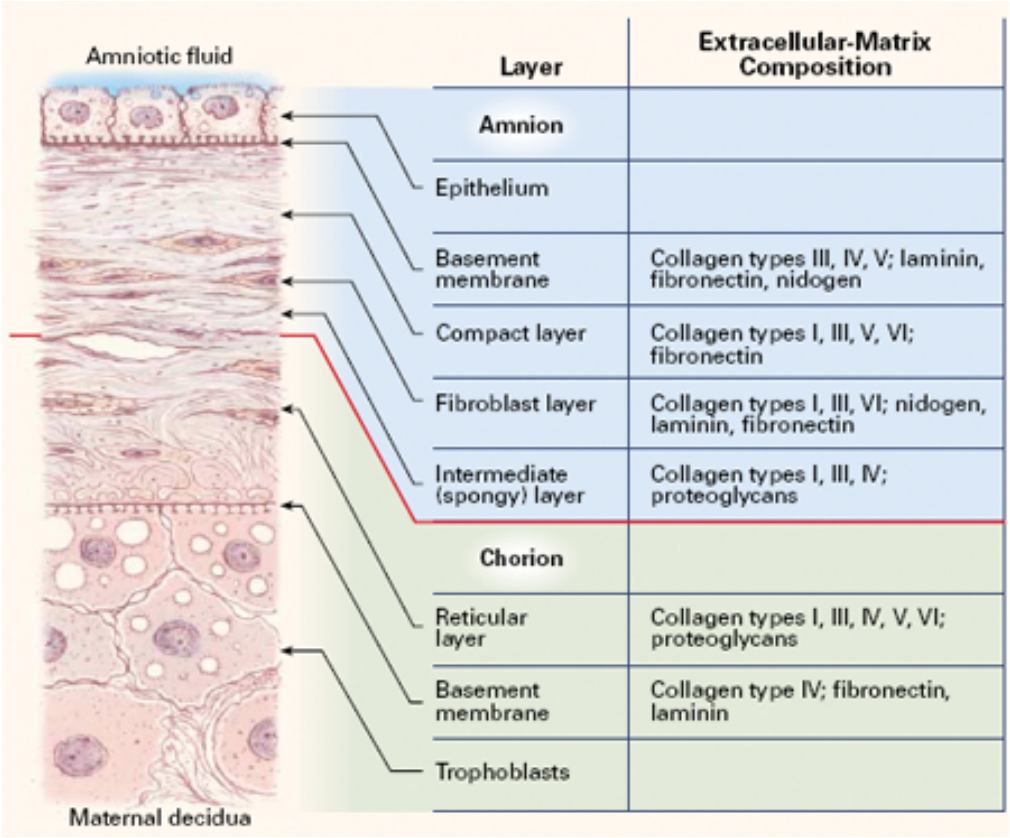

Figure 2 - Layers of the amniotic membrane and chorion (57)

AM is usually 0.02-0.5cm thick, and is consisted of five histologically different layers: epithelium, basement membrane, compact layer, fibroblast layer and spongy layer in the order of from the amnion cavity to the chorion (Figure 2) (5) . The last three layers are sometimes categorized as one, called the avascular stromal layer. The fibroblast layer contains amniotic mesenchymal cells, which are responsible for matrix formation.

Unlike chorion. AM has no blood vessels or nerves and receives its nutrition by diffusion either from the amniotic fluid or the maternal decidua (6).

AM was first used by Davis (7) for skin transplantations in 1910. Since then, AM has been widely applied in different fields of medicine including burn treatment, ocular reconstruction and many types of reconstructive surgery (8). AM's popularity as a scaffold is due to its many desirable characteristics for tissue engineering. Firstly, amniotic epithelial cells (AEC) are pluripotent and clonogenic, making them a good source of stem cells (6). Secondly, studies suggest AM is immunologically inert due to AECs lacking certain surface antigens, such as human leukocyte antigens (HLA) -A, -B, -D and –D related (DR) (9). AECs and amniotic mesenchymal cells also secrete various anti-inflammatory proteins, among them interleukin-1 receptor antagonist (IL-1ra) and IL-10, which inhibit the production of pro-inflammatory factors (10). AM stromal matrix also has a suppressive effect on the IL-1 gene family, which expresses some of the most important pro-inflammatory factors (11). The low immunogenicity of AM reduces the risk of rejection or immune reaction upon transplantation (9). Thirdly, AM acts as a promoter of epithelial migration, adhesion, differentiation, and prevents apoptosis (8). Fourthly, AM is believed to down-regulate transforming growth factor beta (TGF-β) and its receptor, thus reducing fibrosis and scarring (12). AM is also non-tumorigenic and believed to have pain analgesic effects (13).

When used in tissue engineering, the epithelial cells of AM is usually left intact, since the single layer of cuboidal cells is responsible for many of the characteristics that make AM a good scaffold. Studies using acellular AM have also been conducted, in which e.g. fibroblasts and keratinocytes not only adhered to AM acceptably, but also showed good morphology and viability (13,14).

1.3.Stem cells

The two defining characteristics of stem cells are the ability to self-renewal and the capacity to differentiate into multiple cell types. These properties make stem cells very attractive for regenerative medicine, since one cell line can be used to produce endless copies of many cell types. Stem cells have been used successfully in treating e.g. leukemia. Future uses of stem cells include the treatment of a number of degenerative diseases i.e. type I diabetes, multiple sclerosis, Parkinson's disease etc. (15)

The origin of the stem cell defines its potential for differentiation, which can be divided into three categories (Figure 3). Totipotent stem cells (TSCs) can differentiate into any cell of the body and also into trophoblasts, which make up the placenta. Natural TSCs can be found in embryos at the one or two cell stage. Pluripotent stem cells (PSCs) can differentiate into any cell of the body, but not trophoblasts. PSCs can be found in embryos past the one and two cell stage. PSCs also include induced pluripotent stem cells (iPSCs), which are generated from differentiated, somatic cells. Multipotent stem cells can differentiate into any cell of a

specific organ or tissue type e.g. hematopoietic stem cells can differentiate into all blood cells. Multipotent stem cells are often called adult stem cells, since they have been found in various tissues of the adult body. The term somatic stem cell (SSC) is preferred, since multipotent stem cells are formed in the fetal stage of development. One of the most studied multipotent stem cell lineages is mesenchymal stem cell (MSC). MSCs can be found in stroma, such as bone marrow, adipose tissue, synovial tissue, amniotic fluid, placenta and umbilical cord blood, and can differentiate into cell types such as osteocytes, adipocytes, chondrocytes, neurocytes, epithelial and endothelial cells. (15) MSCs were first discovered in bone marrow, presently MSCs are commonly harvested from adipose tissue and umbilical cord blood, since bone marrow collection is invasive and can be painful (16,17)

The use of TSCs and PSCs is ethically controversial since it involves the destruction of human embryos. The same problem is not present when using SSCs, since they can be harvested from consenting individuals without causing them bodily harm e.g. through collection of medical waste such as adipose tissue after liposuction and umbilical cord after birth. (18) Embryonic stem cells (ESCs) can also be problematic since undifferentiated ESCs can form teratomas in the recipient if the transplant material is not completely removed of the undifferentiated ESCs. The downside of SSCs is that they are hard to distinguish from progenitor cells, since adequate assays for SSC recognition has not been developed for a number of tissues. (19)

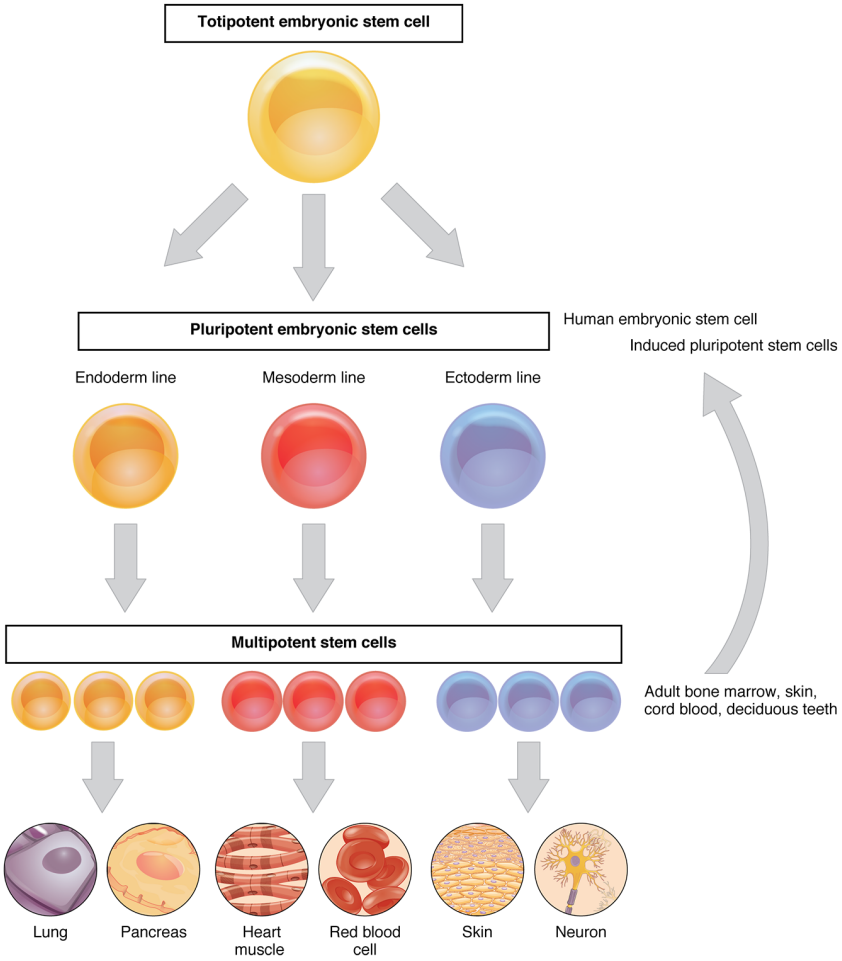

Figure 3 - Hierarchy of stem cells (58)

1.3.1. Adipose-derived stem cells

Adipose-derived stem cells (ASCs) are somatic stem cells found abundantly in the adipose tissue of the adult human body (20). By manipulating the adipose tissue, differentiated adipocytes can be removed, and ASCs can be sourced from the remaining stromal vascular fraction (SVF) (21) .

Since ASCs are of stromal origin (21), they can be classified as mesenchymal stem cells (MSCs). Studies show that MSCs in general have an anti-inflammatory effect on the immune system, which makes them a good candidate for cellular therapy. (22) Compared to the first MSCs found in the bone marrow (BM-MSCs) (23) , ASCs may be a more suitable choice for regenerative medicine. While bone marrow harvesting is painful and can lead to complications, adipose tissue is largely available in the human body, and ASCs can be easily harvested from adipose tissue waste resulting from different surgeries e.g.liposuction. The amount of MSCs that can be collected from bone marrow harvest is also relatively lower than the amount of ASCs that can be collected from adipose tissue (24). While some differences between BM-MSCs and ASCs have been found i.e. gene expression profile and angiogenic potential, the significance of the differences remain uncle1ar (25).

Due to the abundance of ASCs and its multipotent stem cell nature, ASCs are an attractive candidate in the field of wound healing and tissue regeneration. ASCs have been found to secrete almost all of the growth factors that take part in wound healing, i.e. keratinocyte growth factor, vascular endothelial growth factor (VEGF), hepatocyte growth factor, fibroblast growth factor-2, epidermal growth factor, and platelet-derived growth factor, and that the expression of the factors can be increased by preconditioning the cells via hypoxia. The use of ASCs has not been reported to cause significant immunogenicity in hosts, xenografts and allografts alike. Various different ASC delivery methods to wound sites have been tested, including local injection, topical application, collagen gel and fibrin sealant. Consensus on the best method has yet to be reached due to the lack of comparative studies. The application of ASCs in problematic wounds e.g. diabetic, ischemic and radiated tissue has also shown potential. (26)

1.3.2. Human umbilical vein endothelial cells

Human umbilical vein endothelial cells (HUVECs) are harvested after birth from the epithelium of the umbilical vein, which is usually discarded as medical waste. One of the most attractive features of HUVECs is their ability to vascularize engineered tissue constructs, which otherwise will go into necrosis without sufficient nutrient and oxygen supplies. e.g. biomimetic bone tissue has been fabricated using MSCs and HUVECs. (27) In another study, the co-cultivation of MSCs and HUVECs on poly(LLA-*co*-DXO) scaffolds in a 5:1 ratio resulted in a more quiescent phenotype of HUVECs, meaning less proliferation. But at the same time MSCs were found to express significantly more vascular endothelial growth factor A (VEGFa) than

HUVECs alone. The study found that the scaffolds containing both MSCs and HUVECs produced higher density of mature vessels compared to HUVECs alone. It was concluded that MSCs could be a suitable candidate for perivascular cells when engineering blood vessels. (28)

HUVECs have been also used to produce iPSCs, since they lack the ethical issue of ESCs and are better than aged somatic cells, which possess less telomerase activity and contain more nuclear and mitochondrial mutations(29).

1.4.Objectives and expected results

The objective of this study was to create 3D-grafts of AM with adipose tissue and vascular formation through tissue engineering by cultivating ASCs and HUVECs on top of denuded (epithelium removed) AM. The grafts would either allow direct transplantation or enable in vitro examination of adipose tissue. To achieve this, we investigated the cultivation by measuring the expression of AP2, PPAR-γ, vWF and ANGPT1 with quantitative real-time polymerase chain reaction (qPCR). Immunocytochemistry staining, micro-CT and histological analysis were also conducted. The mechanical properties of AM after ASC cultivation were examined through tensile strength tests in Tampere University of Technology.

Vascularization remains an obstacle in tissue engineering, since constructs will go into necrosis without sufficient oxygen and nutrient supply. HUVECs were introduced to the cultivation in hopes of angiogenesis and the co-cultivation along ASCs was expected to promote vessel formation. The tensile strength of AM after cultivation was expected to increase due to the new cell structures.

2. Materials and methods

2.1. Tissues and cells

This study was conducted in accordance of the Ethics Committee of the Pirkanmaa Hospital District, Tampere, Finland (R06045, R15161, R13019).

The amniotic membranes were collected from donor placentas after scheduled C-sections to avoid contamination at Tampere University Hospital. Vaginal deliveries have been shown to increase the possibility of bacterial contamination of AM and thus scheduled C-sections are preferred in general as a harvesting method. The donors were screened for syphilis, HIV and hepatitis B and C.

The ASCs were collected from discarded adipose tissue after surgeries performed at Tampere University Hospital. The ASC donors were otherwise healthy and non-diabetic

The HUVECs were collected from umbilical cords originated from scheduled C-sections at Tampere University Hospital.

2.2. Cultivation of cells on AM

2.2.1. Isolation and culture of cells

Both ASCs and HUVECs were collected using the methods described by Sarkanen et al. (30,31) . The cells were cryopreserved after collection and defrosted when needed. After defrosting, the cells were seeded into 75cm^2 culture flasks along with 10ml of medium. ASCs received basic medium (BM) (Dulbecco's Modified Eagle's Medium/F12 [Invitrogen Ltd.], 5% human serum [Cambrex], 1% L-glutamine [Invitrogen Ltd.], and 1% penicillin-streptomycin mixture [Invitrogen Ltd.]). HUVECs received endothelial medium (EM) (EGM kit [Lonza]: endothelial growth basal medium, 2% human serum, 0,1% VEGF, 0,1% R3-IGF-1, 0,1% GA-1000, 0,1% heparin, 0,01% hEGF, 0,4% hFGF-2, 0,04% hydrocortisone, 0,1% ascorbic acid). The cells were cultured and divided until the desired cell amount was reached. The media were changed twice a week. ASCs usually received a half medium change, since the cells showed great vitality. HUVECs received total medium changes, due to the large amount of dead cells. Despite the large amount of dead HUVECs at each medium change, the cells still proliferated well and had no problem covering the bottom of the culture flask.

Due to the angiogenetic nature of HUVECs, the cells were labeled with ultrasmall superparamagnetic iron oxide (USPIO) particles (diameter approximately 30nm) to enable imaging of the possible vessel formation with micro-CT.

A list of ASC and HUVEC cell lines cultured for this study and their respective analysis can be found in **Error! Reference source not found.**. The expressions of different surface markers of both ASC cell lines are listed in Table 2.

Table 1 - List of cultured cell lines and their respective analysis

Cell line	Analysis
ASC 2/14 P4	qPCR
ASC 2/14 P2 + HUVEC 1 P8 USPIO	Micro-CT + HE histology
ASC 2/14 P4	Tensile strength
ASC 2/14 P3 + HUVEC 1 P10 USPIO x 2 multidish	qPCR (1 multidish) + micro-CT + HE histology (1 multidish)
ASC 2/15 P2 + HUVEC 1 P8 USPIO x 24-well microplate	Immunofluorescence photography (test round, sans AM)
ASC 2/15 P5 + HUVEC 1 P10 USPIO x 4 multidish	qPCR
ASC 2/15 P9 + HUVEC 1 P13 USPIO x 2 multidish	Immunofluorescence photography

Table 2 - Cell surface markers of ASC 2/14 and 2/15

Antigen	Surface protein	Expression 2/14 (2/15)	Fluorophore	Manufacture
CD3	T-cell surface glycoprotein	0,2 (0,5)	phycoerythrin (PE)	BD Biosciences, Franklin Lakes, NJ, USA
CD11a	Lymphocyte function-associated antigen 1	0,6 (0,3)	allophycocyanin (APC)	R&D Systems, Minneapolis, MN, USA
CD14	Serum lipopolysaccharide binding protein	0,3 (0,2)	phycoerythrincyanine (PECy7)	BD Biosciences
CD19	B lymphocyte-lineage differentiation antigen	0,3 (0,2)	PECy7	BD Biosciences
CD34	Siaomucin-like adhesion molecule	35,4 (2,4)	APC	Immunotools, Friesoythe, Germany
CD45	Leukocyte common antigen	1,4 (1,4)	APC	BD Biosciences
CD54	Intercellular adhesion molecule 1	6,6 (7)	fluorescein icothiocyanate (FITC)	BD Biosciences
CD73	Ecto-5'-nucleotidase	96,7 (98,8)	PE	BD Biosciences
CD80	B-lymphocyte activation antigen B7	0,4 (0,5)	PE	R&D Systems
CD86	B-lymphocyte activation antigen B7-2	0,3 (0,4)	PE	R&D Systems
CD90	Thy-1 (T cell surface glycoprotein)	99,7 (99,9)	APC	BD Biosciences
CD105	SH-2, endoglin	97,5 (97,7)	PE	R&D Systems
HLA-DR	Major histocompatibility class II antigens	0,6 (0,5)	PE	Immunotools

2.2.2. Preparation of AM

The AMs used in this study were preserved and prepared by Panu Nordback (M.D. BioMediTech, Tampere, Finland) for his previous project (32). The AM was manually separated from donor placenta and then washed with 0,9% NaCl to remove blood clots and chorion remnants. The washed AM was then cut into suitable pieces and preserved overnight at +4°C in 10% Dulbecco's Phosphate-buffered Saline-solution (DPBS [Lonza Inc.]) containing antibiotics (2.5µg/ml amphotericin B [Invitrogen Ltd.], 5.0µg/ml penicillin [Invitrogen Ltd.], 50µg/ml streptomycin [Invitrogen Ltd.] and 100µg/ml neomycin.). For the removal of the epithelial layer, AM was incubated overnight with 40mg dispase (Invitrogen Ltd.) in 40ml of DMEM/F-12 (Invitrogen Ltd.) solution containing 100U/ml penicillin, 100µg/ml streptomycin and 250ng/ml amphotericin B. After overnight incubation, AM was manually scraped to ensure the complete removal of the epithelial layer, which was verified by microscopic inspection. Dispase-processed AM was washed 10 times with cold DPBS to remove dispase. AM was then put into plastic containers along with DPBS-glycerol solution and cryopreserved at -80° for further use. Before seeding, AM was thawed in +37° and then rinsed with 0,9% NaCl to remove DPBS-glycerol solution in a large Petri dish. Then AM was cut manually into desired sizes using sterile scalpels and tweezers (Figure 4Figure 5). The different sides of AM were indistinguishable with the bare eye, nor were any remarkable differences seen under light microscope. Thus AM was plated at random into the culture dishes, though all wells of the same culture dish were always plated with the AM same side up.

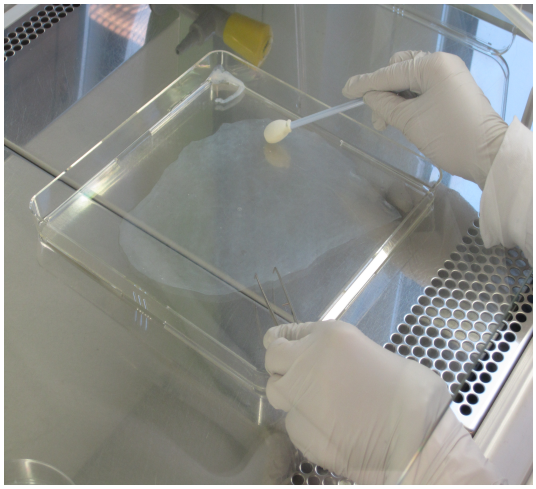

Figure 5 - Spreading of AM before cutting using a large Q-tip

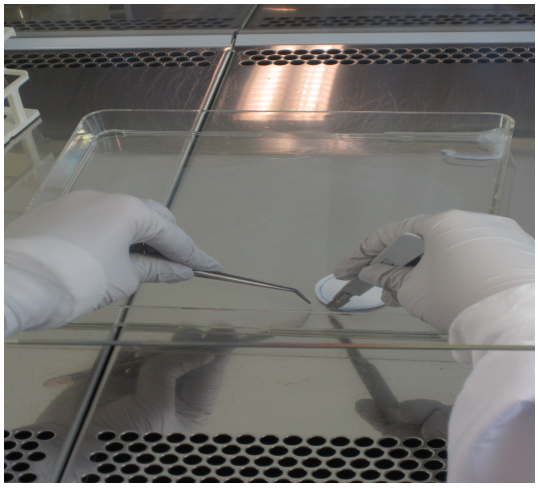

Figure 4 - Cutting of AM, the white paper circle is underneath the Petri Dish and used to model the size of the well of the multidish

2.2.3. Multidish cultivation

Cell cultivation on AM was conducted in untreated 6-well multidishes for three weeks to allow free formation of structures. The bottom of each well was covered entirely with AM. Both rows were plated in the following order: ASC, HUVEC, ASC and HUVEC (Figure 6, Figure 7).

ASC + AM + ADM	HUVEC + AM + ADM	ASC + HUVEC + AM + ADM
ASC + AM + EM	HUVEC + AM + EM	ASC + HUVEC + AM + EM

Figure 7 - Schematic diagram of multidish cultivation

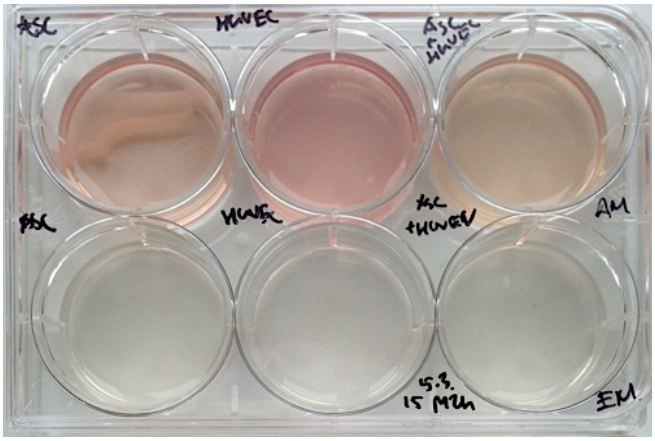

Figure 6 - Multidish cultivation, the top row has received adipose medium and the bottom row endothelial medium

The desired cell amount for ASCs was 20 000c/cm^2 and 10 000c/cm^2 for HUVECs. The area of each well is approximately 1,92cm^2, thus 38 400 of ASCs and 19 200 of HUVECs were seeded into their designated wells, along with 3ml of medium. During seeding and the first day of cultivation, both cell types received the same medium they had in the culture flasks to ensure attachment to AM. ASCs received basic medium and HUVECs endothelial medium and the combination wells received 1,5ml of both media. After one day, the media were discarded and fresh media were applied. The top row received adipose medium (ADM) (Dulbecco's Modified Eagle Medium: Nutrient Mixture F-12 [DMEM/F12, Invitrogen Ltd.], 5% human serum [Cambrex], 1% L-glutamine [Invitrogen Ltd.], 1% penicillin-streptomycin mixture [Invitrogen Ltd.], 1μM dexamethasone [Sigma], 100mM insulin [Sigma], 17μM pantothenate [Sigma], and 33μM biotin [Sigma Aldrich]) and the bottom row endothelial medium. The top row also received 0,005% isobutyl-methylxantine (IBMX) after the first day of seeding to promote ASC differentiation. IBMX were given to the top row only once. The media were replaced twice a week and during those days, the multidishes and wells were photographed to document progress. The multidishes were photographed with a regular camera and the wells were photographed with a light microscope. After three weeks, the AMs were used for: quantitative PCR (qPCR), histological preparation, micro-CT or immunofluorescence imaging. The HUVECs were USPIO-labeled to enable micro-CT imaging.

2.3.Assay methods

2.3.1. RNA isolation, reverse transcription and quantitative real-time polymerase chain reaction

RNA isolation was conducted by using NucleoSpin RNA (Macherey & Nagel GmbH & Co) kit and protocol. After three weeks of cultivation, the amniotic membranes were transferred into individual Eppendorf test tubes and 350µl of RA1 and 3,5µl of β-mercaptoethanol were added into each tube. The tubes were put into -70°C deep freeze before further RNA isolation, due to scheduling reasons. The rest of the RNA isolation was done in one day, according to the protocol. The amniotic membrane and lysisbuffer were first centrifuged through a filter, and then the lysate was homogenized with 350µl of ethanol. The homogenized lysate was centrifuged through a RNA column, after which the lysate was discarded and the column was kept. 350µl of membrane desalting buffer was added to the column and centrifuged. The DNase reaction mixture was prepared by mixing 10µl of reconstituted rDNase and 90µl of reaction buffer for DNase to each sample, after which 95µl of the mixture was applied to each column and incubated in room temperature (RT) for 15 minutes. After incubation, the rDNase was inactivated by the RAW2 buffer and centrifuged. The RAW2 buffer was then washed twice with the RA3 buffer. After the second wash and centrifugation, the column was placed into a nuclease-free collection tube and eluted with 60µl of RNase-free H2O and centrifuged. After elution, the samples were kept on ice, also during reverse transcription and qPCR. The concentration of the eluted RNA was tested with the Nanodrop spectrophotometer, after which the samples containing <4ng/µl of RNA were excluded from reverse transcription.

Before reverse transcription, the RNA samples were diluted to the concentration of 100ng/µl using RNA-free H2O. The samples whose concentration were <100ng/µl were left undiluted. The reverse transcription Master Mix was made with the following recipe for each of the RNA samples: 10 x reaction buffer (6µl), 25 x dNTPs (2.5µl), 10 x random primers (6µl), distilled water (12.5µl) and MultiScribe Reverse transcriptase 3µl. The Master Mix was prepared in a room, which was forbidden from RNA/DNA samples to prevent contamination. 30µl of each diluted RNA sample and 30µl of the Master Mix were pipetted into individual Eppendorf test tubes and then put through PCR. The finished cDNA was then put into a -10°C freezer to await cDNA PCR.

Quantitative real-time polymerase chain reaction (qPCR) was conducted with the Applied Biosystems 7300 Real-Time PCR System. QPCR reveals the amount of a specific DNA sequence in a sample. QPCR operates by the same core principle as regular PCR. By raising the temperature, the DNA double strand opens and allows primers to seek out the desired sequence. The primers are able to anneal to the DNA strand once the temperature is lowered. DNA polymerase on the other hand needs a higher temperature to be able to transcribe a new strand of complement DNA. The aforementioned describes a PCR cycle, which repeats as

many times as programmed. In qPCR, pairing the cDNA (or DNA) sample with specific primers, DNA polymerase, deoxynucleotide triphosphates (dNTPs) and fluorescent dye in alternating temperatures lead to the production of the desired DNA sequence. The fluorescent dye attaches itself to products of the PCR, thus the amount of fluorescence released is directly proportional to the amount of newly synthesized DNA. Since there is an abundant amount of primers to cDNA, the amount of DNA produced in each cycle is directly proportional to the initial amount of cDNA in the sample. The more cDNA the sample contains, the more fluorescence will be achieved in fewer cycles. The threshold for fluorescence detection is set, and it is measured how many cycles are needed to reach the threshold (quantitation cycle, Cq). Standard samples, whose DNA concentration are known and vary from each other, are also put through qPCR. The Cq of the test samples is compared to the Cq of the standards, and the initial amount of cDNA can be calculated. (33)

In this study, the qPCR Master Mix for each sample was: SYBR green Master Mix (7.5µl, Applied Biosystems), forward primer (0.5µl), reverse primer (0.5µl) and distilled water (5.5µl). The cDNA sample was diluted in the ratio of 1:1 with distilled water before the Master Mix was added. Each qPCR plate included one no template control (NTC) in the form of distilled water and five standards of different concentration. Each sample, NTC and standard was pipetted into three individual qPCR wells to minimize pipetting-related errors.

The genes that were quantified in this study were: RPLP0, AP2, PPAR-γ, vWF and ANGPT1. RPLP0 encodes a component of the 60S subunit of ribosomes, making it a housekeeping gene, which is expressed in virtually all cells. Since RPLP0 expression is so common, it is used as a reference gene, to which the expressions of other genes are compared. (30) AP2 encodes adipocyte protein 2, a carrier protein for fatty acids, thus AP2 expression is usually abundant in adipocytes(34). PPAR-γ encodes peroxisome proliferator-activated receptor gamma, a nuclear receptor involved in adipocyte differentiation (30). The vWF gene encodes von Willebrand factor, a glycoprotein involved in hemostasis. VWF is both produced and stored in HUVECs. (35) Lastly, ANGPT1 encodes angiopoeitin-1, a glycoprotein involved in angiogenesis (31). The sequences used can be found in Table 3.

Table 3 - Oligonucleotide sequences used for qPCR

Gene	Accession number	Primer
Human ribosomal protein, large, P0 (hRPLP0)	NM_001002	Forward 5'-AAT CTC CAG GGG CAC CAT T-3' Reverse 5'-CGC TGG CTC CCA CTT TGT-3'
Human adipocyte protein 2 (AP2)	NM_001442	Forward 5'-GGTGGTGGAATGCGTCATG-3' Reverse 5'-CAACGTCCCTTGGCTTATGC-3'
Human peroxisome proliferator-activated receptor gamma (hPPAR-γ)		Forward 5'-CAGTGTGAATTACAGCAAACC-3' Reverse 5'-ACAGTGTATCAGTGAAGGAAT-3'
Human angiopoietin 1 (hANGPT-1)	NM_001146	Forward 5'-TGCAAATGTGCCCTCATGTTA-3' Reverse 5'-TCCCGCAGTATAGAACATTCCA-3'
Human von Willebrand factor (hvWF)		Forward 5´-AGAAACGCTCCTTCTCGATTATTG-3' Reverse 5'-TGTCAAAAAATTCCCCAAGATACAC-3´

2.3.2. Ultrasmall superparamagnetic iron oxide labeling and micro-CT

USPIO labeling always took place three days prior to seeding. On the first day, HUVECs were detached from the culture flasks and counted. The protocol used in this study called for 1000µg of USPIOs to 100 000 cells. The USPIO stock was 25mg/ml and the amount needed was always first diluted to a to working solution of 1mg/ml with EM. The amino acid poly-D-lysine (PDL) was used to ease uptake of USPIO particles into the cells. (36) The ratio of PDL to HUVECs was 3750µg to 100 000 cells. The PDL was mixed with the working solution of USPIO and EM. The mixture was incubated in RT for 30 minutes and gently vortexed every 10 minutes. After incubation, the working solution was diluted to a final solution of 200µg/ml with EM. The HUVECs were put into new culture flasks along with the final solution. After two days of incubation in +37°C, the USPIO-PDL-EM was replaced with EM, and left to incubate for one more day in +37° before plating.

The AMs that were subjected to micro-CT and histology were fixed with paraformaldehyde (PFA) after three weeks of culturing. The AMs were put into individual Eppendorf test tubes and 1ml of 4% PFA was added and incubated in RT for one hour. After incubation, the PFA was replaced with 1ml of 70% ethanol. The test tubes were put into +5°C storage while waiting for further analysis.

Kalle Lehto (M.Sc., Tampere University of Technology) performed the micro-CT. Micro-CT employs the same technology as regular computer tomography, using X-ray to construct 3D cross-section images. The micro-prefix means that the resulting image can show micrometer range detail. Prior to the micro-CT, the

AMs were put into scaffolds made out of 1ml medical syringes. The barrel of the syringe was cut from the bottom and the tip of the plunger was also cut off and put back in the barrel backwards, so that the rubber end was pointing outwards. The AM was then put into the barrel, and another, fully intact plunger was inserted. The end result being the AM between two rubber ends of plungers inside the barrel (Figure 8). The AM was left as much space as it needed to rest freely. The space surrounding the AM was filled with 9% NaCl drawn via the tip of the syringe to prevent drying. The syringe was imaged in an upright position with parafilm stretched over the tip of syringe. All equipment, including the knife used to cut the syringes and the pieces of the syringe were wiped down with 90% ethanol to prevent pieces of metal transferring to the AM.

Figure 8 - Micro-CT scaffold

2.3.3. Histology

The same AMs that underwent micro-CT were prepared into histology slides by Sari Kalliokoski (BioMediTech). After micro-CT, the samples were stored in 70% ethanol until histology. In short, the samples were dehydrated, embedded in paraffin, and sectioned at 5-mm thickness. The sections were rehydrated and stained with hematoxylin and eosin (H&E). Hematoxylin acts as a basic dye, meaning it binds to acidic structures such as the nucleic acids, coloring them dark blue or purple. Eosin on the other hand acts as an acidic dye, binding to basic compounds, such as proteins and coloring them either pink, red or orange.

2.3.4. Immunofluorescence microscopy and photography

After three weeks of culture, two of the multidishes were subjected to immunofluorescence microscopy and photography. Immunofluorescence is based on the mechanism of antibodies attaching to their respective antigens, and when fluorescent-labeled antibodies are used, the emission can be detected through light microscopy. The different stains were photographed separately through their respective filters with the Olympus IX51 fluorescence microscope. Afterwards the photos were processed and combined using Photoshop.

The staining was done with anti-von Willebrand factor antibody (anti-vWF AB), DAPI (4',6-diamidino-2-phenylindole) and phalloidin. DAPI binds strongly to the A-T regions of the DNA, thus revealing the

nucleus of cells. In this study, DAPI was colored blue in the final pictures. Phalloidin on the other hand binds to filamentous actin (F-actin), which is a part of the cytoskeleton of cells. In this study, phalloidin was colored red in the final photos.

As mentioned previously, vWF is a glycoprotein involved in hemostasis. HUVECs have been shown to both produce and store vWF (35). The staining of vWF was done indirectly by first labeling the AM with a primary rabbit anti-vWF antibody (ThermoFisher). Then the fluorescence was achieved with a secondary goat anti-rabbit antibody (ThermFisher). In this study, vWF was colored green in the final pictures.

Before staining, the AMs were fixed with 0.1% Triton X-100 (Sigma) in 4% of PFA. 500µl of fixing solution was applied to each well to cover the bottom. After 15 minutes of incubation in RT, the fixing solution was discarded and the AMs were washed four times with DPBS. 1ml of DPBS was applied to each well after washes and the multidishes were wrapped in plastic and put into +5°C storage to wait for staining. Staining itself was done during the course of two days. On the first day, the DPBS was discarded and 300µl of blocking solution of 1% bovine serum albumin (BSA) was applied to each well and left to incubate in RT for one hour. The blocking solution is meant to block the nonspecific epitopes to prevent the staining antibodies to attach to them, thus reducing background staining noise. After blocking, the primary antibody incubation of vWF with rabbit anti-vWF antibody was done with the ratio of 1:500 antibody to 1% BSA. Other concentrations were tested earlier, including 1:100 and 1:200, but 1:500 was deemed sufficient enough. The multidishes were left to incubate in the primary antibody solution overnight in +5°C storage wrapped in tin foil. On the second day, the anti-vWF antibody was washed with DPBS. The secondary antibody incubation of goat anti-rabbit (1:800 of antibody to 1% BSA) and the direct staining of phalloidin (1:300 to 1% BSA) were done at the same time. The secondary incubation was left for one hour in RT (in the fume cupboard due to the toxic nature of phalloidin). After incubation, the wells were washed with DPBS and DAPI was applied in the ratio of 1:2000 to PBS (phosphate-buffered saline-solution). DAPI was incubated in RT for 5 minutes, after which it was washed with DPBS. DPBS was discarded and 1ml of Milli-Q purified water was added to each well, after which the wells were photographed using the Olympus IX51 fluorescence microscope.

2.3.5. Tensile strength test

AM was first laid onto a sheet of sterile nitrocellulose (NC) paper to keep it from balling up, making it easier to maneuver. Then the AM and the underlying paper were cut into suitable pieces to be placed into custom-made cultivation scaffolds made of Teflon to keep it smooth and flat for the tensile strength test. The scaffolds are 2x7cm rectangles, consisting of a front and back piece, the AM and NC paper was placed between the pieces. The effect of cell cultivation on the mechanical properties of AM was tested with ASCs alone, the desired amount of cells was also 20 000c/cm^2. The front piece has an opening in the center, where ASCs were seeded along with basic medium (Figure 9). The opening in the scaffold is approximately 1,5cm^2,

thus 30 000 ASCs were plated to each AM. The scaffolds were placed in Petri dishes filled with enough basic medium to cover AM. The measurement points were one day after plating, one and three weeks after cultivation.

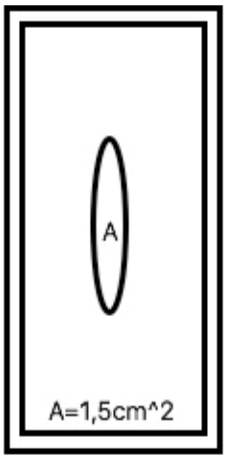

Figure 10 - Culture scaffold for tensile strength test

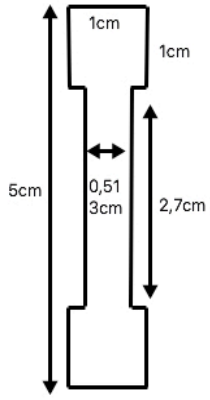

Figure 9 - Measurements of tensile strength test sample

The actual measurements took place in Tampere University of Technology and were assisted by Laura Johansson (M.Sc. Tampere University of Technology). The AM and paper were removed from its scaffold and cut into a dog biscuit shape (1x5cm) using a punch stencil (Figure 10). The dog biscuit shape provides larger end pieces, which were inserted into the clamps of the tension test machine. This arrangement was made to ensure that the pressure is focused in the middle of the sample, where the ASCs are. At each measurement point, two blank AM (along with nitrocellulose paper) were also measured as controls. The NC paper is suitable for the tension test, because it breaks easily and its elasticity is significantly lower than AMs, thus not affecting the tensile strength of AM.

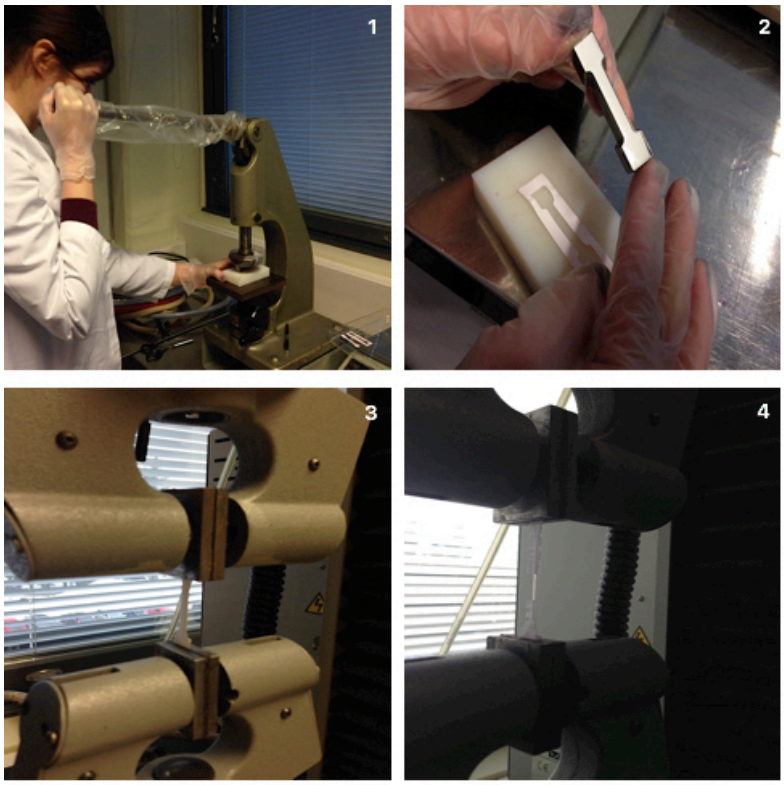

Figure 11 - Tensile strength test –

1: cutting of AM into dog biscuit shape

2: punch stencil and cut AM + NC paper

3: AM in between tensile test machine

4: the desired way of nitrocellulose paper breaking in the middle, leaving AM intact

3. Results

3.1.Light microscopy

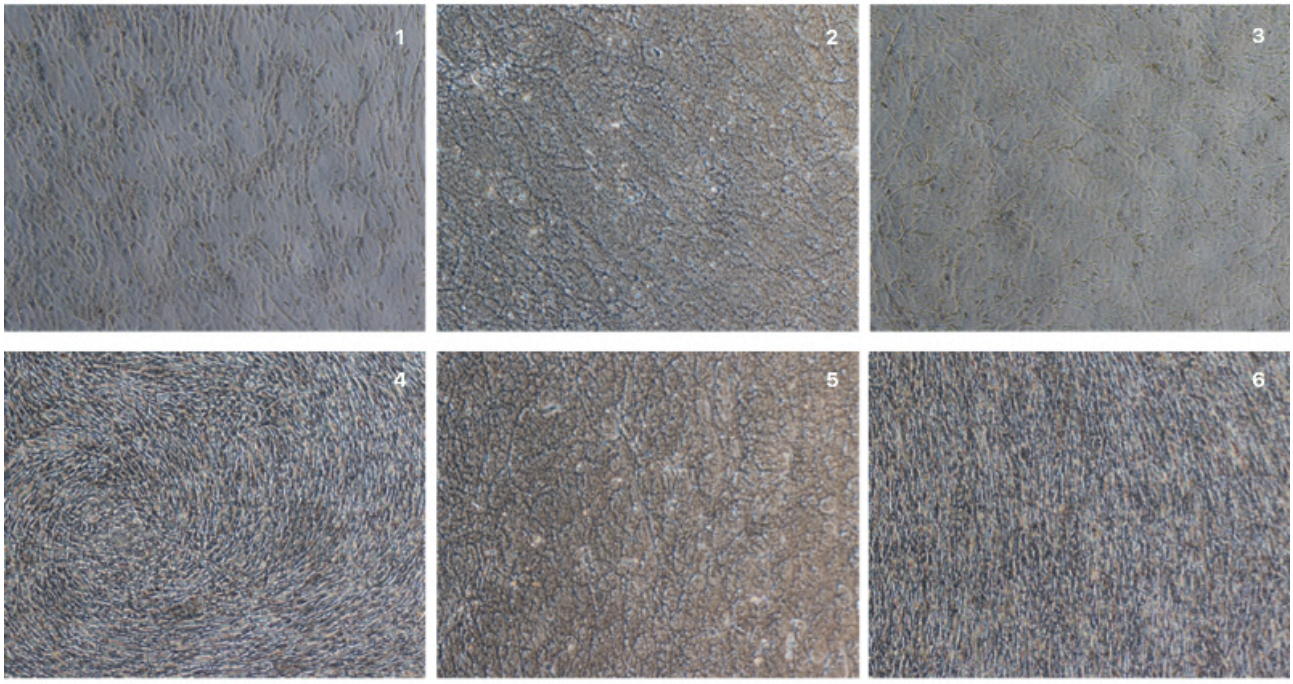

Figure 12 - Multidish cultivation week 1 x4 zoom, first row was in ADM, second row was in EM; 1: ASC + ADM; 2: HUVEC + ADM; 3: ASC + HUVEC + ADM; 4: ASC + EM; 5: HUVEC + EM; 6: ASC + HUVEC + EM

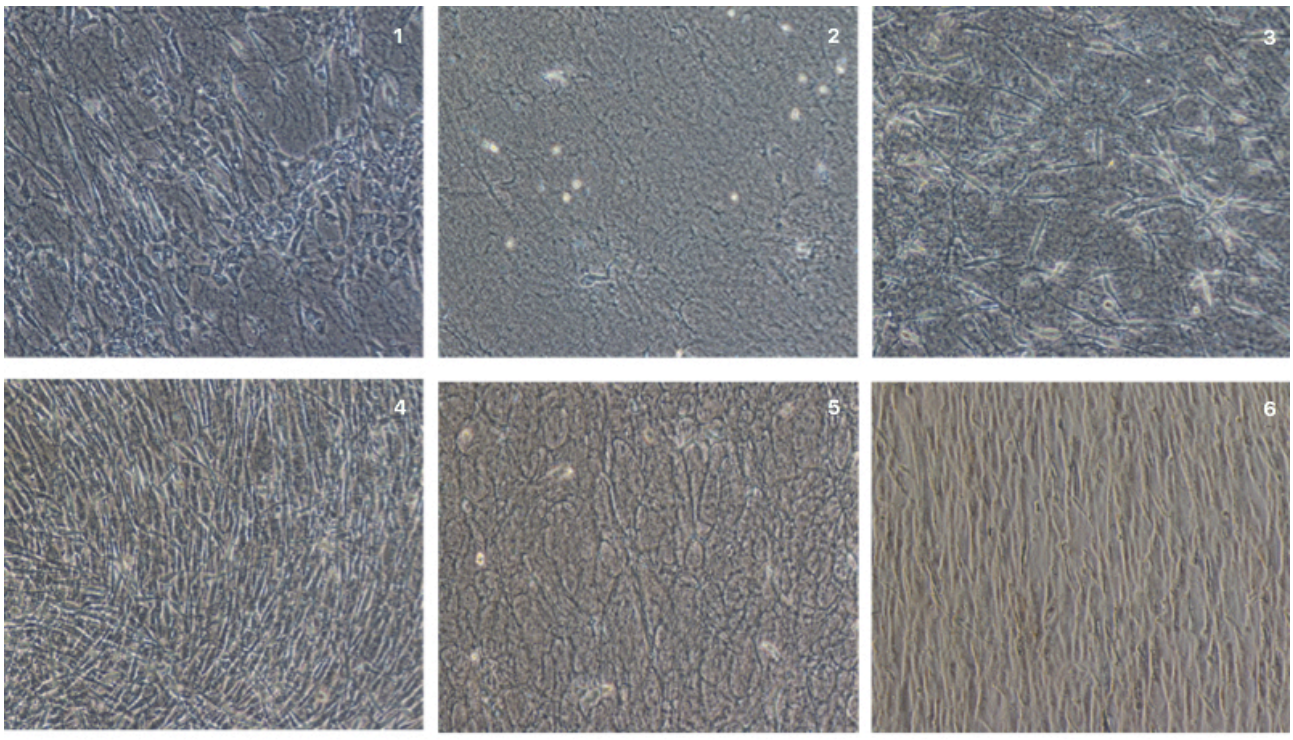

Figure 13 - Multidish cultivation week 1 x 10 zoom, first row was in ADM, second row was in EM; 1: ASC + ADM; 2: HUVEC + ADM; 3: ASC + HUVEC + ADM; 4: ASC + EM; 5: HUVEC + EM; 6: ASC + HUVEC + EM

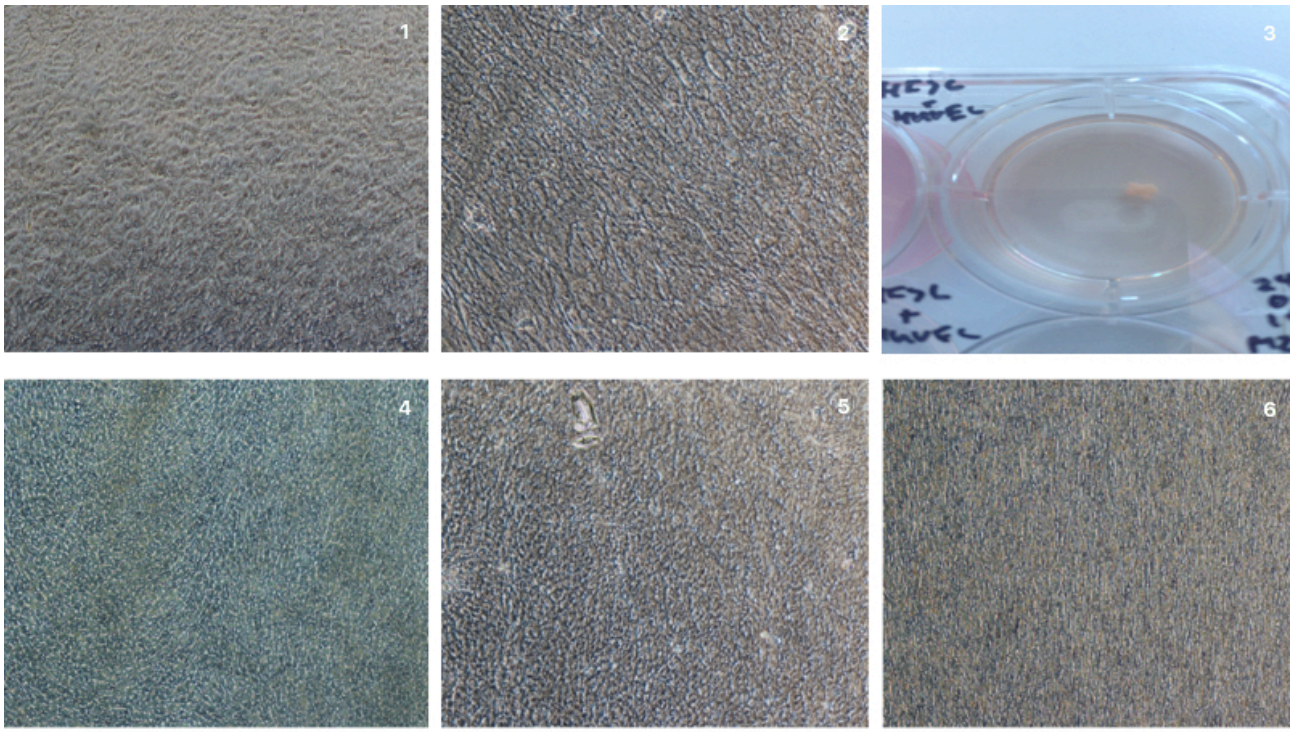

Figure 14 – Multidish cultivation week 3 x4 zoom, first row was in ADM, second row was in EM; 1: ASC + ADM; 2: HUVEC + ADM; 3: ASC + HUVEC + ADM; 4: ASC + EM; 5: HUVEC + EM; 6: ASC + HUVEC + EM; note ASC + HUVEC in ADM had shrunk, thus couldn't be photographed with microscope

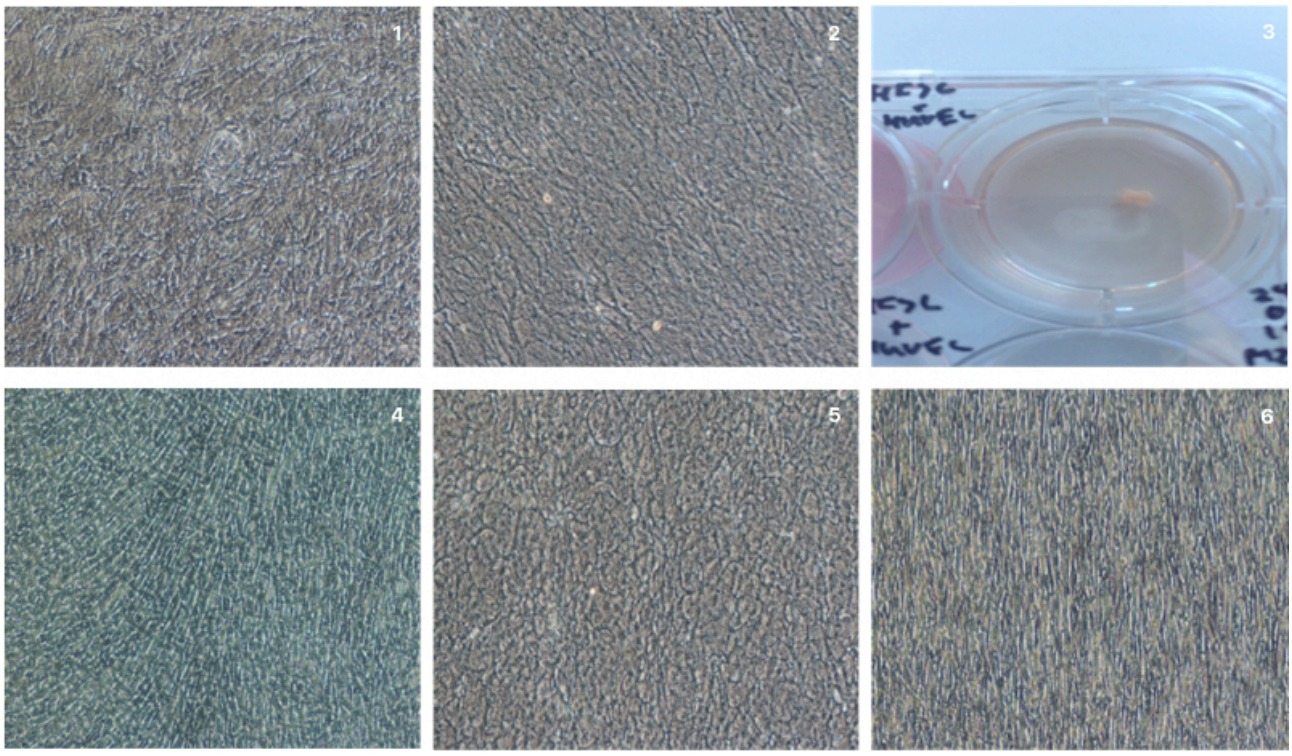

Figure 15 - Multidish cultivation week 3 x10 zoom; first row was in ADM, second row was in EM; 1: ASC + ADM; 2: HUVEC + ADM; 3: ASC + HUVEC + ADM; 4: ASC + EM; 5: HUVEC + EM; 6: ASC + HUVEC + EM; note ASC + HUVEC in ADM had shrunk, thus couldn't be photographed with microscope

The multidishes were photographed with a Zeiss light microscope with white balance during every medium change, each well was photographed using x4 and x10 zoom. The photos featured in this study were of the ASC 2/15 P5 and HUVEC 1 P10 cell lines. There were four multidishes featuring the same cell lines and all of them underwent RNA extraction and qPCR after three weeks of culture.

During the first week of culture (Figure 12 and 13), cell formations could be seen in all the wells. ASCs demonstrated the typical MSC morphology, meaning a small cell body with long, thin, polygonal processes (37). ASCs could be seen in abundance in all the wells it was plated in (1, 3, 4 and 6 of both Figure 12 and 13), showing great vitality even in EM. In ADM, the ASCs appeared to grow randomly (1 of both Fig.12 and 13), but in EM, the ASCs seemed to grow in a tightly coiled spiral (4 of both Figure 12 and Figure 13). In the wells containing only HUVECs (2 and 5 of both Fig.12 and 13), there was thought to be tube formation, since distinct line structures could be seen. However, when compared to images of AM alone (Figure 16), the HUVEC wells looked very similar to the denuded AM, and we struggled to distinguish any cell structures with the bare eye. Curiously, the intense, natural pattern of AM was not seen in ASC wells, where ASCs could be easily spotted. In the combination wells (3 and 6 of both Fig.12 and 13), the spindle-shaped ASCs were easy to detect. Some HUVECs could be seen in the combination wells cultured in ADM (3 of both Fig.12 and 13), unlike the long and thin ASCs, HUVECs were small and round, cobblestone-like(38). HUVECs were again hard to distinguish in the combination wells cultured in EM (6 of both Fig.12 and 13). Interestingly, the ASCs of the combination wells cultured in EM grew tightly packed in vertical lines.

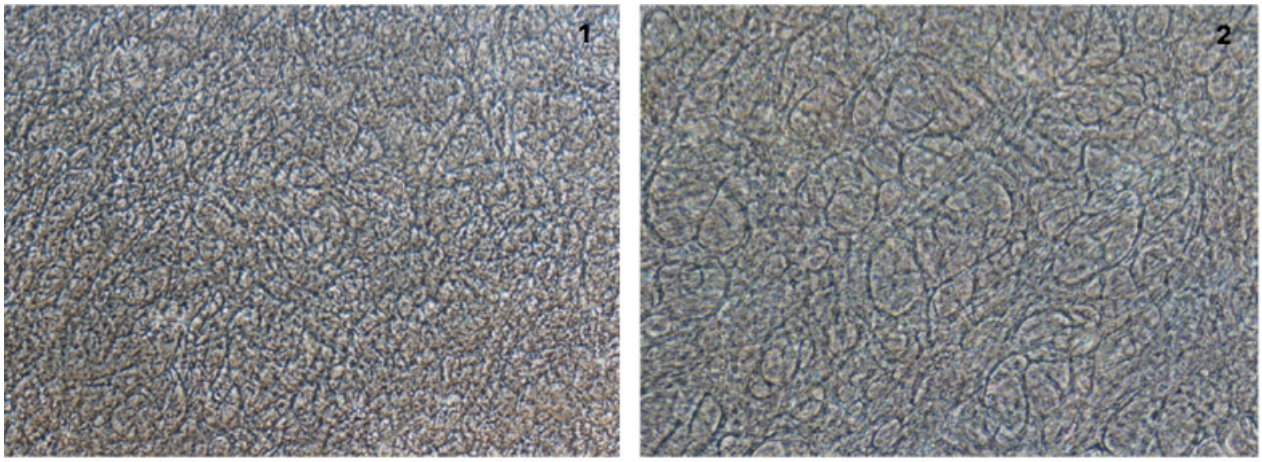

Figure 16 - Light microscopy photos of denuded AM; 1: x4 zoom; 2: x10 zoom

By the third week of culture, ASCs had proliferated in both ADM and EM (1 and 4 of both Figure 15 and Figure 16). ASCs continued to grow randomly in ADM (1 of both Fig.14 and 15), the spiral-like growth in EM wasn't as obvious as before, but a certain level of waviness could still be detected (especially in Fig.15.4). HUVECs were still difficult to distinguish from bare AM, nor was there much difference compared to the photos taken during the first week (2 and 5 of Fig.14 and 15). ASCs of the combination wells in EM maintained their vertical growth and became even more tightly packed (6 of both Fig.14 and 15). The AM of combination wells in ADM had balled up, making photography impossible (3 of both Fig.14 and 15). The shrinking of AM in the combination wells cultured in ADM was repeated in all of the

multidishes. Contraction occurred nearly always in the ASCs in ADM wells and the combination wells in EM, but wasn't as rapid and complete as in the combination wells in ADM. Milder shrinkage was seen in the ASCs in EM wells as well. The only wells where AM remained undisturbed for three weeks were the HUVECs-only wells. The shrinking of AM could be a sign of cell proliferation activity.

3.2.QPCR

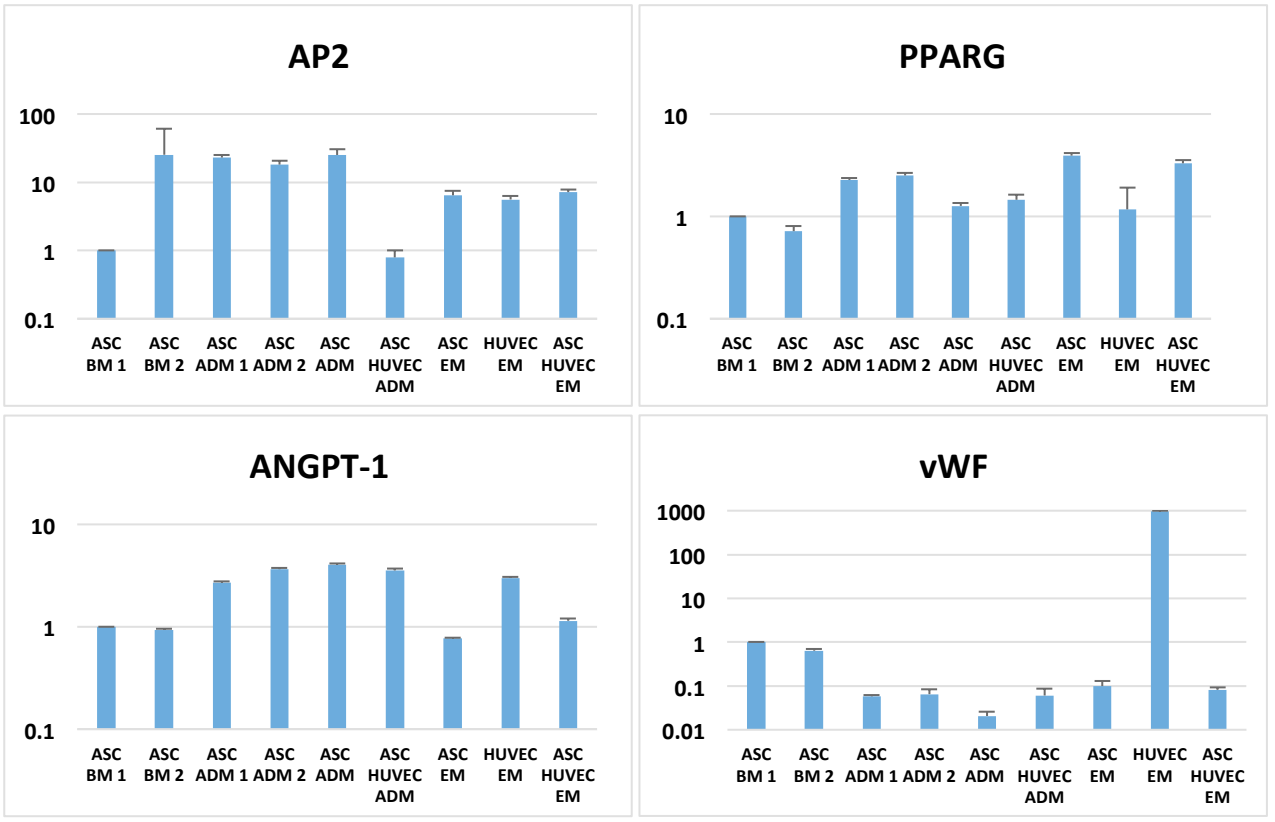

Figure 17 - First set of qPCR results in logarithmic scale. Results presented in brackets are actual figures.

ASC BM 1 used as a control sample. All results represent one sample. ASC=adipose stem cell, HUVEC=human umbilical vein entdothelial cell, BM=basic medium, ADM=adipose medium, EM=endothelial medium.

After RNA isolation, the nucleic acid concentration of each sample was tested with the Nanodrop 2000 spectrophotometer (Thermo Scientific). Although a concentration over 100ng/µl was desired, the results ranged from 0,6-182,49ng/µl. HUVECs in ADM had to be excluded from DNA translation in both sets, due to poor RNA concentration (0,6-1,69ng/µl). In the first set of results, every column represents one sample; the samples were of the ASC 2/14 P4, ASC 2/14 P3 and HUVEC P10 cell lines (Figure 17). In the second set, every column is the average result of 4 samples; the samples were the same ones featured previously in the light microscopy photographs (Figure 18). All results were compared to RPLP0, a housekeeping gene.

AM with ASCs in BM was also included in the first set of qPCR as a control, with the relative expression of the ASC BM 1 sample marked as one for each gene (Figure 17).

In the second set, one sample of ASCs in ADM was used as the control sample (ASC ADM 1), thus ASC ADM is the average of the three other samples. The results are displayed in logarithmic scale due to the different magnitude of results (Fig.18). Note the y-axis of vWF in the first set begins with 0.01 whereas 0.1 is the first value in all of the other results (Fig.17).

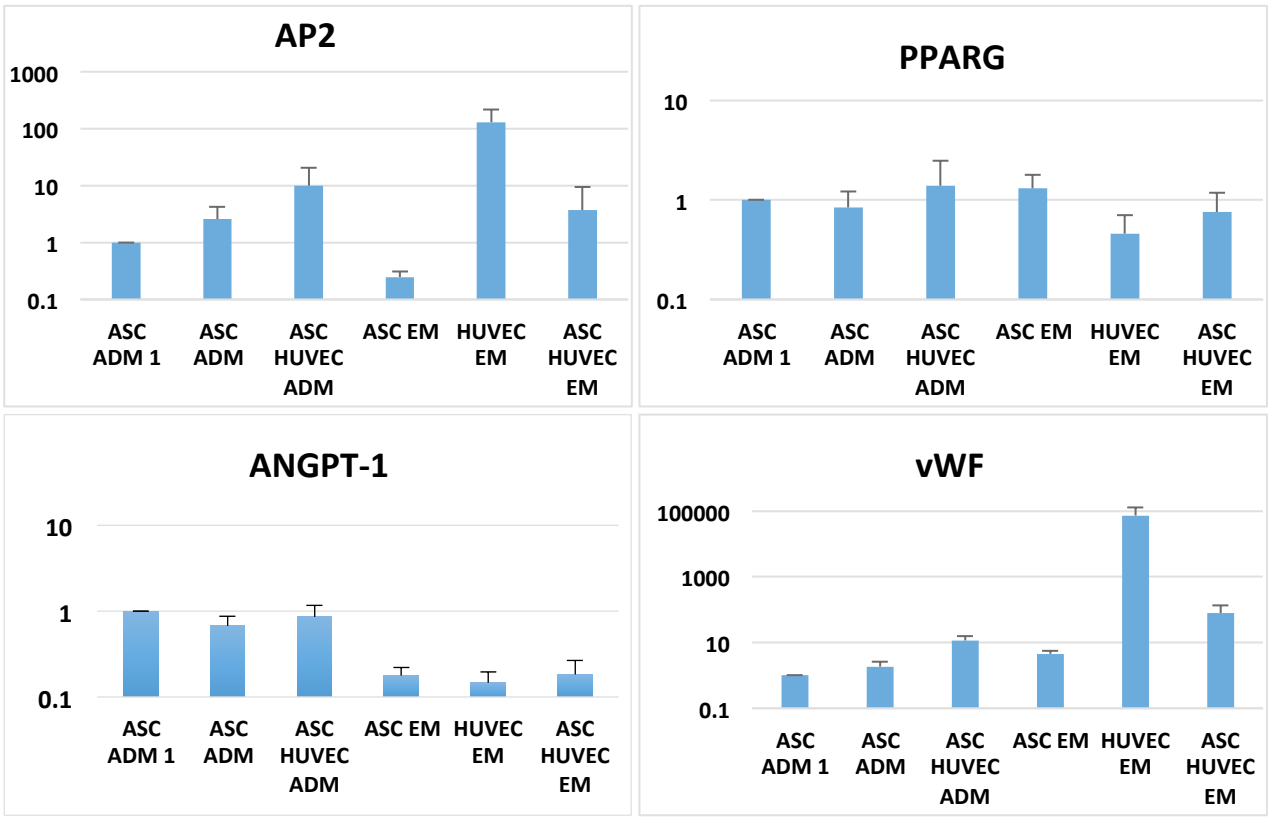

Figure 18 - Second set of qPCR results with logarithmic scale. Results presented in brackets are actual figures.

ASC ADM 1 used as a control sample. ASC ADM1 represents one sample, ASC ADM the average of three samples and the rest an average of four samples.

ASC=adipose stem cell, HUVEC=human umbilical vein entdothelial cell, BM=basic medium, ADM=adipose medium, EM=endothelial medium.

AP2 and PPAR-γ are both adipocyte-related genes and were expected to be abundant in the samples containing ASCs. In the first set, the highest relative expression of AP2 was in the ASCs in BM and ADM (18,1-25,3) samples. The non-control sample of ASCs in BM for some reason expressed AP2 25 times more than the control sample of ASCs in BM. Both samples of ASCs in BM behaved similarly in the expression of other genes. Compared to the control sample, the lowest concentration of AP2 was found in the combination well in EM (0.79). The other samples in EM (ASCs, HUVECs and combination) showed more AP2 expression (5.6-7.2) than the control sample of ASCs in BM. The expression of AP2 did not correlate with the expression of PPAR-γ, which was expressed fairly the same in all samples (0.72-3.9). Compared to ASCs

in BM, samples of ASCs in EM (ASCs and combination) expressed PPAR-γ 3-4 fold (3.9 and 3.3), ASCs in ADM expressed PPAR-γ twice as much as the control sample (2.3-2.5) with the exception of one sample (ASC ADM Fig.17; 1.3). ASCs in BM and HUVECs in EM expressed PPAR-γ approximately the same amount as the control sample (0.72 and 1.2). In the second set, the most AP2 expression was found surprisingly in HUVECs in EM (131.4), whose expression was over tenfold the expression of the combination sample in ADM (10.0), which came second. There are no previous reports on AP2 expression by HUVECs. The expression of AP2 in ASCs in ADM was mild compared to the first set (2.6). PPAR-γ expression was rather similar also in the second set (0.46-1.4), the most expression was found in the combination sample in ADM (3.3) and ASCs in EM (3.9). HUVECs in EM showed the least expression of PPAR-γ (0.46) compared to the control sample.

ANGPT-1 and vWF are genes involved in angiogenesis and hemostasis, and were expected to be widely expressed in samples containing HUVECs. In the first set, the most ANGPT-1 expression was seen in two of the ASCs in ADM samples (3.6-4.0), with the combination sample in ADM coming in a close third (3.5) (Fig.17). HUVECs in EM was only in fourth place (3.0), the combination well in EM faired only a little better than the control sample (1.1). The expression of ANGPT-1 did not correlate with the expression of vWF. VWF was expressed the most in HUVECs in EM, as expected (971.5). The result was thousandfold the vWF expression in all other samples (<1). In the second set, the control sample demonstrated the most expression of ANGPT-1. Out of the other samples, the combination sample in ADM expressed the most ANGPT-1 (0.86) by a minor lead over ASCs in ADM (0,67) (Fig.18), mirroring the results of the first set. HUVECs in EM and the combination sample in EM demonstrated significantly less expression than in the first set (<0.2). HUVECs in EM again expressed the most vWF (73982.9), the result repeated the thousandfold lead to the next greatest expression by the combination sample in EM (78.4). The combination sample in ADM also demonstrated a tenfold vWF expression compared to the control sample (11.6). The expression of vWF in other samples than HUVECs in EM was not seen in the first set of qPCR.

In conclusion, the most replicable result was of vWF. HUVECs in EM clearly expressed the most vWF in both sets of qPCR, as expected. HUVECs in EM produced the least PPAR-γ in the second set, and also in the first set, if the non-control ASCs in BM sample is excluded. The overall expression of PPAR-γ and ANGPT-1 was rather similar between samples in both sets of qPCR. The combination sample in ADM and ASCs in ADM seemed to produce the most ANGPT-1 in both sets, although HUVECs in EM also had notable expression in the first set, it was not seen in the second set. The dramatic AP2 expression of HUVECs in EM in the second set was not echoed by the first set. While the combination well in ADM had notable expression of all four genes (except vWF in the first set), it has to be noted that the expression of ANGPT-1 and vWF in both sets do not differ significantly from the expression found in ASCs in ADM, leading one to question how much of the expression can be credited to ASCs. The combination well in EM showed notable expression in both sets of adipocyte-related genes, but out of the vascularization-related genes, only vWF expression was seen clearly in the second set of qPCR.

3.3.Immunofluorescence photography

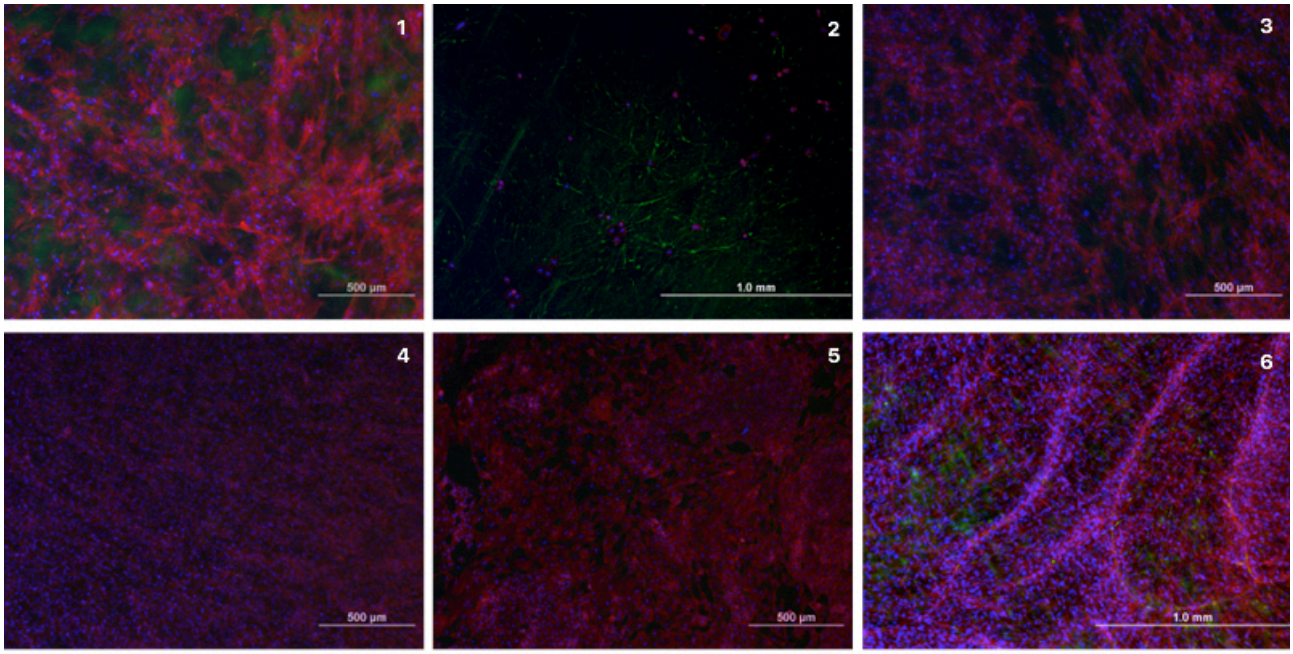

Figure 19 - Immunofluorescence pictures x 4, each well stained with DAPI (blue), phalloidin (red) and vWF (green); 1: ASC + ADM; 2: HUVEC + ADM; 3: ASC + HUVEC + ADM; 4: ASC + EM; 5: HUVEC + EM; 6: ASC + HUVEC + EM

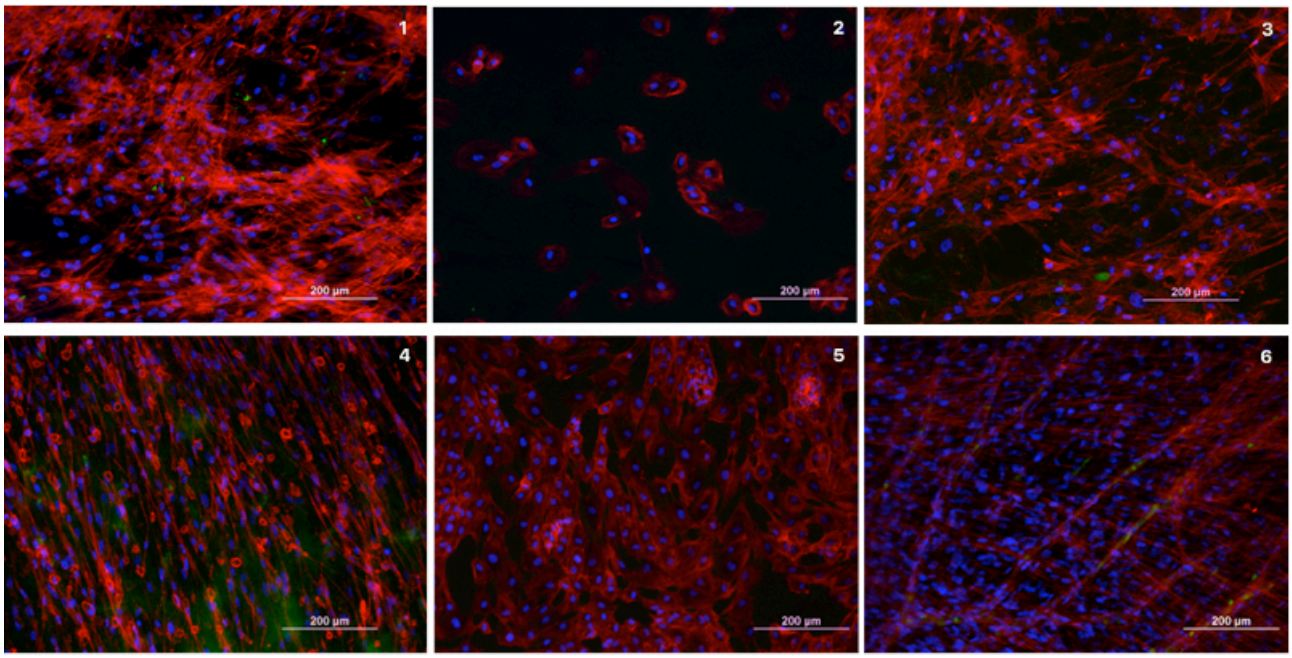

Figure 20 - Immunofluorescence pictures x 10, each well stained with DAPI (blue), phalloidin (red) and vWF (green); 1: ASC + ADM; 2: HUVEC + ADM; 3: ASC + HUVEC + ADM; 4: ASC + EM; 5: HUVEC + EM; 6: ASC + HUVEC + EM

One multidish featuring ASC 2/15 P9 and HUVEC 1 P13 was subjected to immunofluorescence photography after three weeks of culture. Each well was stained with DAPI, phalloidin and vWF, and photographed with x4 (Figure 19) and x10 (Figure 20) zoom. Each stain was photographed separately using

an Olympus IX51 fluorescence microscope. Afterwards the pictures were combined and colored with Photoshop. The blue color of DAPI shows the nucleus, the red color of phalloidin shows the cytoskeleton and vWF was colored green.

A lot of nuclei could be seen in all wells except HUVECs in ADM (Figure 19.2 & Figure 20.2), which could be anticipated due to the lack of RNA during RNA isolation. Phalloidin-stained cytoskeleton could also be seen in each well. Green specks of vWF could only be seen weakly in a few of the wells. We expected to see vWF in the HUVEC wells, and some vWF activity was seen in the HUVECs in ADM well (Fig.19.2) and the combination well in EM (Fig.19.6) with x4 zoom. However the results were not replicable with x10 zoom. This is curious, since according to qPCR, vWF was greatly expressed in the HUVEC in EM wells and the combination in EM wells.

The ASCs in ADM (Fig.19.1 & 20.1) seemed to grow randomly, like in the light microscopy pictures. A weak spiral-like growth could be seen in the ASCs in EM well with x4 zoom (Fig.19.4). The spiral-pattern was lost in x10 zoom, but the cytoskeleton of different cells were still parallel to each other, showing a regularity not seen in other wells (Fig.20.4); this was also comparable to the light microscope pictures taken of this well (4 of Fig.12-15). Some interesting line formations could be seen in the combination well in EM, visible in both x4 (Fig.19.6) and x10 (Fig.20.6) zoom. The lines seemed to be formed by nuclei and their respective cytoskeleton. The light microscope photo of this well showed the cells growing in a vertically tightly packed manner; this was not seen in the immunofluorescence pictures.

3.4.Hematoxylin-eosin stained histology

Two HUVECs in EM samples first underwent micro-CT and were then prepared into H&E stained histology slides. They were of HUVEC 1 cell line, passages 8 and 10. The histology pictures (**Error! Reference source not found.**) featured in this study were photographed with the same Zeiss light microscope that was used to document the multidish cultivation. The samples were photographed with x10 zoom and white balance; both pictures represent the same sample.

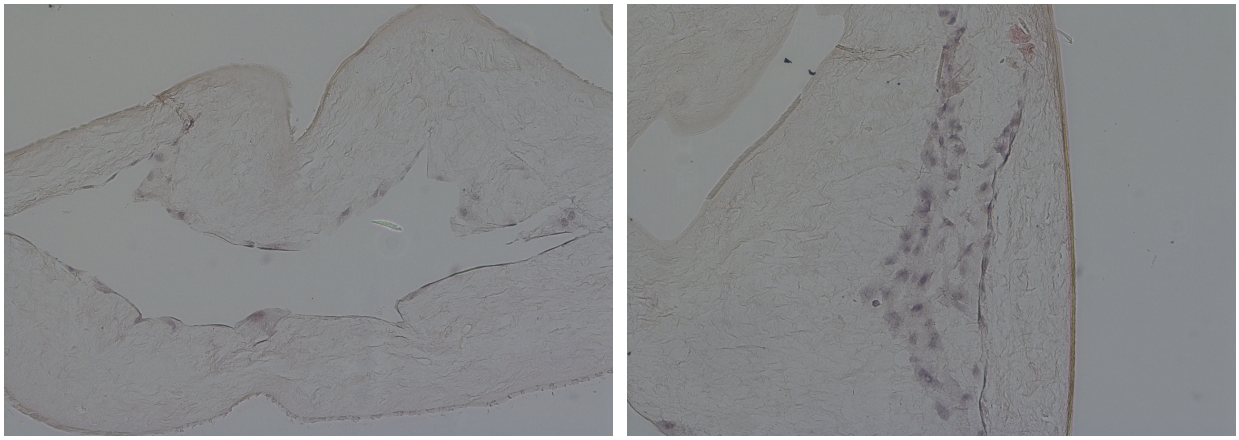

Figure 21 - H&E stained AM + HUVEC + EM x 10 zoom

In the left picture is a cross-section of AM, cells could be seen lining the one side of the AM. The cells seemed to cover the entirety of AM in a single layer of cells. In the right picture, a cluster of cells could be seen in the AM matrix. Due to the straight edge seen on the right side of the cluster and the fraying seen on top, it could be assumed that the cells detached from the surface of AM during slicing. Interestingly, the detached cluster seemed to grow in many layers, as opposed to the picture on the left.

3.5.Micro-CT

The same samples that underwent H&E staining and histology slicing were first subjected to micro-CT. Figure 22Figure 23 consists of six stills of HUVECs in EM samples in micro-CT, together the pictures show the AM in 360° view. The HUVECs were labeled with USPIO-particles during cultivation to enable micro-CT to detect possible tube formation. In the first session of micro-CT (Figure 22), a large, metallic cluster was seen near the top of the AM sample. We concluded that the metal was a remnant from the blade used to make the syringe scaffold. For the next session of micro-CT, the scaffold was wiped down carefully with 90% ethanol to avoid contamination. Phase contrast was also applied to enable a better view of the USPIO-particles. Unfortunately, the USPIO-particles remained unseen. A speck of red could be seen near the top of the AM, but when taken into consideration that 1000µg of USPIO was applied to every 100 000 HUVECs, it seemed odd that only one particle would remain after three weeks. The existence of HUVECs in EM cultivated on AM can be seen in the immunofluorescence (Fig.19.5 and 20.5) and the H&E stained histology pictures (Fig.21). One explanation could be that the HUVECs eventually pushed the foreign particles out during the three-week cultivation. Due to the large amount of dead HUVECs during initial cultivation, this scenario could be plausible. Another explanation could be that since the USPIO-particles were nano-sized, they couldn't be detected in micro-CT, which is used to detect micro-sized details. But there have been studies, in which micro-CT successfully detected UPSIO-particles. (39)

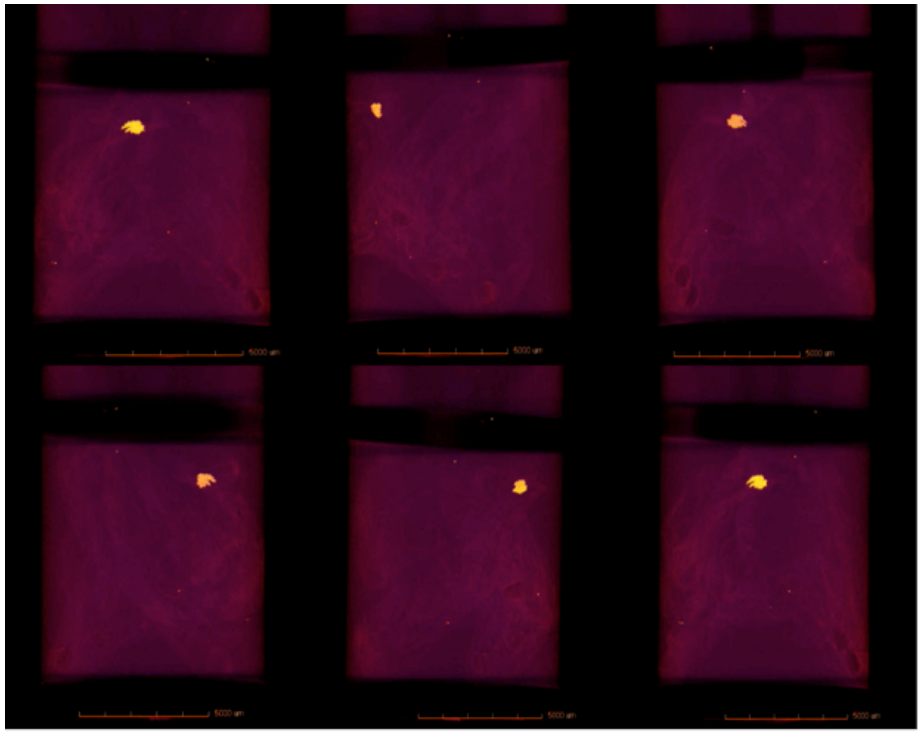

Figure 22 - Micro-CT stills of AM with HUVEC + EM

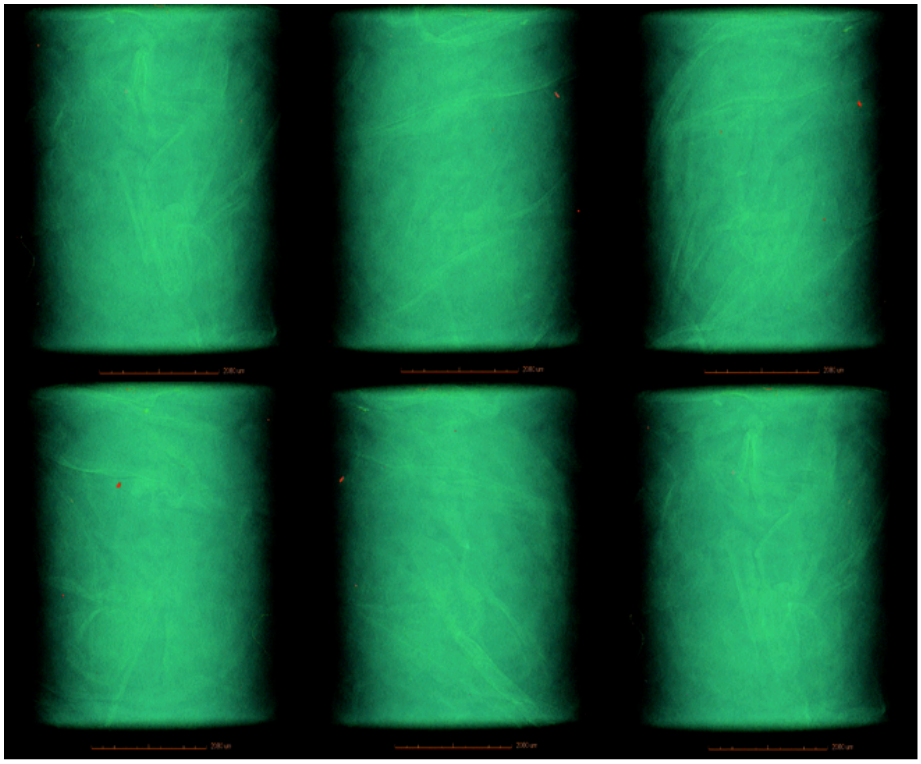

Figure 23 - Phase contrast micro-CT stills of AM with HUVEC + EM

3.6.Tensile strength

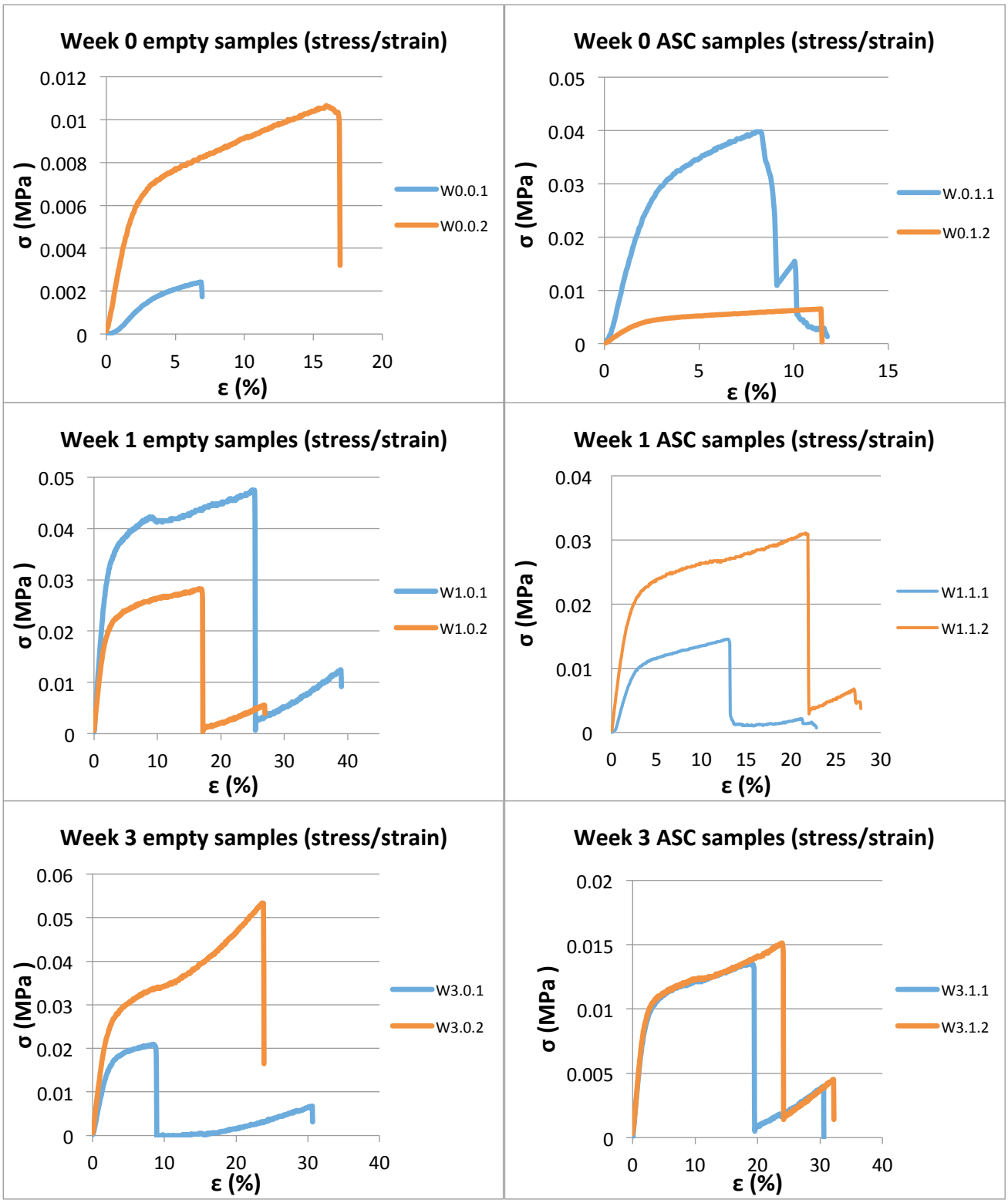

Figure 24 - Stress/strain graphs of tensile strength test, top left: week 0 empty samples, top right: week 0 ASC samples; middle left: week 1 empty samples; middle right: week 1 ASC samples; bottom left: week 3 empty samples; bottom right: week 3 ASC samples

The samples were numerically labeled, the first number represents the specific time point (week 0, week 1 and week 3), the second number represents whether ASCs were cultivated (0 meaning only AM, 1 meaning AM and ASCs), the last number differentiates the two samples of the same kind tested at each time point (sample 1 and sample 2).

The AMs cultivated on top of NC paper in the Teflon scaffolds were subjected to tensile strength tests after one day (week 0), one week and three weeks of culture in BM. At each time point, four samples were tested, two empty samples with only AM and two samples of AM cultivated with ASCs.

The AMs and NC paper were cut into dog biscuit shapes, whose wide ends were put between the clamps of the uniaxial tension test machine. The machine registered the elongation of the sample and the corresponding applied force. Engineering strain was calculated by determining the percentage of elongation to the original length of the AM sample, which was 3cm. Engineering stress was calculated by the dividing the force needed to break the AM by the cross-section area of the thinner middle piece. The area was dependent on the thickness of the particular AM sample, which was measured together with the NC paper, after which the thickness of the NC paper (1.33mm) was subtracted from the measurement. The thickness of the AM acted as the height of the area, and the width of the area was the same as the width of the thinner part of the dog biscuit, 0,5cm. The fracturing of NC paper and then AM were too low-energy to be registered by the tensile test machine, thus the breaking points were determined manually based on the data.

Figure 24 features line graphs of each sample; in the graphs engineering stress is plotted against engineering strain, note the axis scale varies between the samples. On the left side of Figure 24 are the empty AM samples and on the right are the samples containing ASCs cultured on AM. Two empty samples and two ASC samples were tested during each time point. The samples were numerically labeled, the first number represents the specific time point (week 0, week 1 and week 3), the second number represents whether ASCs were cultivated (0 meaning only AM, 1 meaning AM and ASCs), the last number differentiates the two samples of the same kind tested at each time point (sample 1 and sample 2). The same labeling carries on in Figure 25, which depicts the individual properties of each sample.

In Figure 24, all except the top two panels and the second empty sample of week three show two distinct peaks, the first one being the breaking point of the NC paper, and the second being the breaking point of AM. In the samples whose graph only show one peak, AM had broken simultaneously with the NC paper. In the first sample with ASCs of week 0, AM first tore incompletely along the NC paper, and broke into two a while later, thus the jagged shape of the graph. The overall shape of the two-peaked graphs look very similar, despite the samples tearing from different locations: the samples of week one broke near the middle, the samples of week three broke near the bottom.

Figure 25 shows the individual properties of each sample, note the thickness of AM and engineering stress were displayed in logarithmic scale, due to the significantly different magnitude of results. Most of the AMs ranged between 0.01-0.02 mm in thickness, but the first empty sample of week 0 was 0.22 mm thick. The top four samples in applied force all broke along the NC paper, which can also be seen in Fig.24; more force was needed to break the NC paper than AM. The thickest AMs (week 0 empty samples and the week 1 second ASC sample) all broke at the same time as the NC paper, so any advantage of thickness was not seen. The elongation was obviously larger in the samples that broke independently from NC paper, ranging between

3.01-11.7mm. Since engineering strain is elongation divided by 30mm, the engineering graph correlates completely with the elongation graph. After one week of culture, the first empty sample elongated more than the other week one samples (11.7 mm versus 6.4-8.1 mm). After three weeks of culture, there was no significant difference in elongation nor applied force between the empty samples and the ASC samples. The ASC samples elongated more on week three than week one (9.4 mm average versus 7.7mm average). The week three ASC samples though, were thicker than the week one samples, which could be also seen in engineering stress; even though week three samples elongated more, week one samples endured more engineering stress (4.5E-3 MPa average versus 4.2E-3 MPa). The effects of ASC culture on AM was hard to determine due to the premature breaking of week 0 AMs, though it could also be a sign of improved tensile strength through culture, that AM broke independently from NC paper after at least one week of culture.

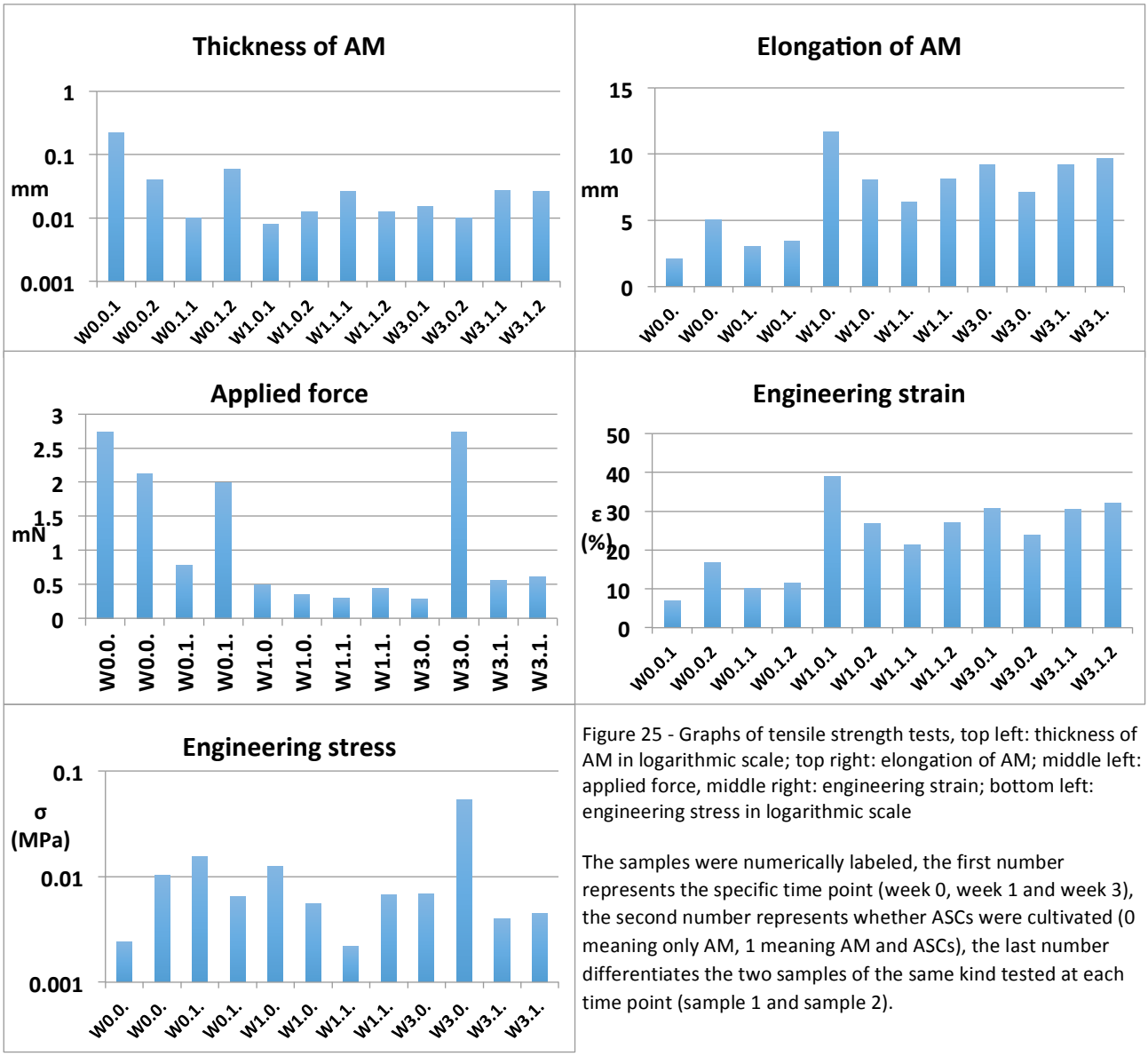

Figure 25 - Graphs of tensile strength tests, top left: thickness of AM in logarithmic scale; top right: elongation of AM; middle left: applied force, middle right: engineering strain; bottom left: engineering stress in logarithmic scale

The samples were numerically labeled, the first number represents the specific time point (week 0, week 1 and week 3), the second number represents whether ASCs were cultivated (0 meaning only AM, 1 meaning AM and ASCs), the last number differentiates the two samples of the same kind tested at each time point (sample 1 and sample 2).

4. Discussion

This study had three main focuses: will ASC cultivation lead to adipose formation on AM, will the co-culture of ASCs and HUVECs on AM lead to tube formation, and how does the culturing of cells affect the tensile strength of AM. The topics will be discussed separately.

4.1. Adipose formation

The cultivation of MSCs on AM has been done many times before, often with bone marrow MSCS, e.g. for the purposes of corneal (40,41) and dermal wound healing (42). In Roux et al.'s study, cultivation of BM-MSCs and ASCs on the stromal side of AM was compared to each other. The stromal side was chosen due to the difficulties of removing the epithelial layer of AM and the lack of standardization of the process. The cells were cultured with α-modified Eagle's medium (α-MEM) and 5% human platelet lysate. Researchers found that MSCs adhered 100% to AM even with higher seeding dose (up to 180 000 cells/cm^2), which was remarkably better than to plastic (at 180 000 cells/cm^2, 24% for BM-MSCs and 27% for ASCs). Both types of MSCs remained viable after 15 days of culture, seen by using Alamar blue assay. ASCs were not induced to form adipose tissue. (43)

In this study, while ASCs showed great viability in all the wells they were plated, the typical morphology of lipid droplet accumulations in differentiated adipocytes (44) weren't seen in any of the microscope pictures (Fig. 12-15, 19 and 20). All ASC wells received IMBX after one day of plating; the IMBX was left for 24 hours before it was removed. The lack of droplet formation could be due to the ambiguous adipocyte-related gene expression found in qPCR. In the first set of qPCR (Fig.17), AP2 was clearly expressed more in the ASCs in ADM samples, the same was not seen in the second set (Fig.18), where HUVECs in EM expressed the most AP2. PPAR-γ expression did not differ between ASC and HUVEC samples in both sets of qPCR. To the best of my knowledge, there are no previous studies conducted on whether ASC cultivation on AM will lead to adipose formation. In this study 0,005% IMBX was used to induce adipogenesis, other cultivation media and induction agents have been proven to affect ASC proliferation and differentiation and should be looked into in future studies (45).

4.2.Angiogenesis and tube formation

Angiogenesis is crucial for wound healing and tissue engineering, since necrosis will occur without sufficient oxygen and nutrient supply (27). Thus HUVECs were introduced to the cultivation in hopes of added angiogenesis. MSCs have been shown to promote angiogenesis when co-cultivated with HUVECs, producing more vessel-like structures than HUVECs alone. In Kachgal's and Putnam's study, ASCs and HUVECs were cultivated in 3D fibrin matrices using the same endothelial medium kit as in our study (46) . In Jiang et al.'s study, amniotic MSCs were co-cultivated with HUVECs, also in 3D fibrin matrices, using alfa-MEM (minimum essential medium eagle with alpha modification) (47). Both chose MSCs for their proteolytic abilities, which are needed in every step of angiogenesis. Both came to the same conclusion, that the co-culture of MSCs and HUVEC produced more vessel-like structures than HUVECs alone. (46,47) Merfeld-Clauss et al. co-cultured 2D monolayers of HUVECs with ASCs in endothelial growth basal medium and 5% fetal bovine serum. They hypothesized that HUVECs-only vessels are unstable and need a layer of stabilizing mural cells. The inclusion of ASCs did lead to longer-lasting vessel networks. (48)

In this study, some cord formation was seen in the immunofluorescence pictures of the combination wells in EM (Fig.19.6 and 20.6). The expression of vWF in combination samples in EM was seen in the second set of qPCR (Figure 18). ANGPT-1 expression in combination samples in EM was the same as the control sample in the first set of qPCR (Figure 17) and actually lower than the control sample in the second set of qPCR (Figure 18). The similar angiogenic gene expression between HUVECs and ASCs doesn't necessarily mean HUVECs demonstrated poor angiogenic activity, since ASCs have been shown to express angiogenic factors, including VEGF and interleukin-8 (49) .

In Lin et al's study, ASCs were cultivated on dopamine-coated electrospun fiber mats. Angiogenic properties of ASCs were tested by cultivation in DMEM with 2% fetal bovine serum with 50ng/ml of VEGF as an induction agent. ELISA results showed, that ANGPT-1 and vWF expression increased over time (1,3 -1,7 times between day 3 and day 7), meaning ASCs do express ANGPT-1 and vWF. (50) VEGF was a component of the EM used in this study, but ASCs in EM did not show more angiogenic gene expression than ASCs in AM. This could be due to the different concentration of VEGF used in this study (0,1%). In Kingham et al's study, ASCs were stimulated with basic fibroblast growth factor and platelet-derived growth factor for two weeks, after which RT-PCR revealed significantly increased VEGF-A and ANGPT-1 expression. Unstimulated ASCs also released high levels of VEGF-A (20,92 ng/ml). The study also included HUVEC cultivation with either conditioned medium from stimulated ASCs or directly alongside stimulated ASCs, both leading to significantly more tube formation (length of continuously linked cells: 1,696µm in control sample, 2,346µm in conditioned medium and 3,667µm in direct contact with stimulated ASCs). (51) The combination wells in EM of this study did show some cord-like formations (Fig.19.6 and 20.6) in immunofluorescence photography, but the lack of green vWF in the pictures cast doubt on whether the cords seen in the immunofluorescence pictures are tube formation.

Based on the light microscopy pictures, HUVECs did not proliferate well in ADM. The same result could be seen in the immunofluorescence pictures and by the lack of RNA during RNA isolation. It could be concluded that ADM is not a suitable medium for HUVECs. Even though the combination samples in ADM showed promising cell viability in all of the assays, it is difficult to distinguish how much of the results are due to ASCs rather than HUVECs. For example, when the expression of ANGPT-1 and vWF are compared between the combination samples in ADM and ASCs in ADM, the results are quite similar (Fig.17 and 18). HUVECs alone in EM proliferated well (Fig.19.5 and 20.5), a lot of vWF expression was seen in qPCR. The combination well in EM was full of cells (Fig.12.6, 13.6, 19.6 and 20.6), but again, it was difficult to distinguish the amount of ASCs to HUVECs. The co-cultivation of ASCs and HUVECs did affect morphology; in ADM, AM balled up completely, in EM, the cells grew tightly packed in vertical lines (3 and 6 of Fig.14 and 15). In summary, the true amount of HUVECs in combination wells was hard to determine; angiogenic activity was hard to interpret, due to angiogenic nature of ASCs, making it hard to compare to and distinguish from the expression of HUVECs. The USPIO-labeling of HUVECs was supposed to help identify them in micro-CT, and would have helped to determine the true amount of HUVECs in the combination samples. But as seen in the stills of micro-CT (Fig.21 and 22), none USPIO-particles were detected, either due to the expulsion of the particles by HUVECs or the sensitivity of the micro-CT.

On the other hand, poor expression of angiogenic genes could be due to the properties of the AM. As previously mentioned, AM is a popular material for ocular reconstructive surgery, namely for its anti-angiogenic properties e.g. inhibition of endothelial cell growth and suppression of corneal neovascularization (8,40,41). All four groups of tissue inhibitors of metalloproteinase (TIMPs) have been found in the stromal layer of AM, produced by both the amniotic epithelial and mesenchymal cells. TIMPs inhibit matrix metalloproteinases, which are critical in angiogenesis. Other antiangiogenic proteins have also been found in AM, but TIMPs are also secreted by amniotic mesenchymal cells and can be found in the stromal layer. (10) Since the AMs used in this study were denuded, we could exclude the effects of amniotic epithelial cells, but the TIMPs of the stromal layer could be the reason behind the lack of angiogenesis. This could explain why ANGPT-1 was expressed less than expected. Also, in Choi et al's study, HUVEC adhesion to AM was not as good as HUVEC adhesion to plastic (54.7% vs. 78.3%) (52) .

4.3.Tensile strength

The tensile strength tests were inconclusive due to the limited number of samples and the premature breakage of a couple of the samples. Even though it seems that the ASC samples elongated a little more after three weeks of culture than one week of culture, the sample size was simply too small to draw any conclusions (Fig.25). The vast variations in AM thickness (0.008 to 0.22mm) and the fact of the thickest samples tearing along NC paper made it difficult to determine the relationship between AM thickness and tensile strength. In a review study done in 2009, the average thickness of AM with epithelium was estimated

to be 50μm (0.05mm) (53) . The average thickness of denuded AM in our study was 0.04mm, which seems credible, despite the discrepancy among the samples. The location of where the harvested AM situated in the amnion cavity did not seem to affect AM tensile strength (53) . In Oyen et al's study, the average peak force AM with epithelium could withhold without breaking was 1.57 ± 0.62N, and the average elongation was 4.10 ± 0.40mm (54) . The average peak force in our study was 1.1N and 0.47N when the prematurely torn samples were excluded. The average elongation in our study was 6.90mm, which may insinuate that denuded AM is more flexible. In Amensag et al's study, human vascular smooth muscle cells were cultivated on AM up to 40 days, after which AM strips were put between the clamps of an uniaxial tension test machine. Engineering stress was shown to progressively decrease over time (2,35 MPa day 0 and 0,40 MPa day 40). (55) This study also came to the same conclusion (4.5E-3 MPa average day 0 versus 4.2E-3 MPa average day 21). Amensag et al had a higher cell density than our study (60 000 cells/cm^2) (55) compared to 20 000 ASCs/cm^2, which could explain the more dramatic decrease in engineering stress. The other studies on fetal membrane tension strength measured AM alone, without any support like the NC paper used in this study (53,54) . NC paper was however necessary for this study, since ASC cultivation would have caused AM to ball up without the Teflon scaffold, and the placement of AM onto the scaffold was impossible without NC paper.

4.4.Conclusion

The objectives of this study were to cultivate 3D-grafts of AM with adipose tissue and vascular formation. In summary, adipose formation on AM was not seen, nor were certain tube formations. Tensile strength tests proved to be the opposite of our hypothesis, engineering stress actually decreased with time, though this was in line with previous findings (55)

The main weakness of this study was the inconsistency of results; more sets of each analysis assay are needed to achieve reliable results. Even though the stromal side of AM has also been shown to be a valid scaffold for cultivation (43) a way of identifying the different sides of AM should be adopted for future studies, for the sake of consistency. Since the thickness of AM samples varied significantly, more samples are needed for reliable results. Tensile strength testing without nitrocellulose paper should also be attempted, since other tensile strength tests are mainly done with bare AM (54-56). The amount of viable HUVECs in combination wells should also be determined, since it was difficult to tell based on qPCR and photography. The possibility of nanotomography (nano-CT) should be explored, if USPIO particles can't be detected even in nano-CT, the problem of HUVECs expelling USPIO particles should be looked into.

To maximize possible tube formation, different induction agents should be looked into e.g.basic fibroblast growth factor and platelet-derived growth factor (51), to stimulate the angiogenic capacity of ASCs. The

same applies to ASCs as well, different cultivation medium and induction agents should be tested in future studies.

In conclusion, AM is a feasible scaffold for cell cultivation, ASCs proliferated well in both media and combinations, HUVECs were certainly abundant in EM, perhaps also in the combination wells. Co-cultivation of ASCs and HUVECs induced changes in morphology, even though tube formation was not achieved. The Teflon scaffold and NC paper enabled tensile strength measurements, which were technically a success. A larger sampling is needed for conclusive results.

5. References

(1) Langer R, Vacanti JP. Tissue engineering. Science 1993 May 14;260(5110):920-926.

(2) Langer R, Vacanti J. Advances in tissue engineering. J Pediatr Surg 2016 Jan;51(1):8-12.

(3) Vacanti JP, Langer R. Tissue engineering: the design and fabrication of living replacement devices for surgical reconstruction and transplantation. Lancet 1999 Jul;354 Suppl 1:SI32-4.

(4) Sadler TW, Langman J. Langman's medical embryology. 12th ed. ed. Philadelphia (Pa.): Lippincott William & Wilkins; cop. 2012.

(5) Bourne G. The FÅ“tal Membranes: A Review of the Anatomy of Normal Amnion and Chorion and Some Aspects of Their Function. Postgrad Med J 1962 Apr;38(438):193-201.

(6) Niknejad H, Peirovi H, Jorjani M, Ahmadiani A, Ghanavi J, Seifalian AM. Properties of the amniotic membrane for potential use in tissue engineering. Eur Cell Mater 2008 Apr 29;15:88-99.

(7) Davis J. Skin transplantation with a review of 550 cases at the Johns Hopkins Hospital. Johns Hopkins Med J 1910;15(307).

(8) Mamede AC, Carvalho MJ, Abrantes AM, Laranjo M, Maia CJ, Botelho MF. Amniotic membrane: from structure and functions to clinical applications. Cell Tissue Res 2012 Aug;349(2):447-458.

(9) Hori J, Wang M, Kamiya K, Takahashi H, Sakuragawa N. Immunological characteristics of amniotic epithelium. Cornea 2006 Dec;25(10 Suppl 1):S53-8.

(10) Hao Y, Ma DH, Hwang DG, Kim WS, Zhang F. Identification of antiangiogenic and antiinflammatory proteins in human amniotic membrane. Cornea 2000 May;19(3):348-352.

(11) Solomon A, Rosenblatt M, Monroy D, Ji Z, Pflugfelder SC, Tseng SC. Suppression of interleukin 1alpha and interleukin 1beta in human limbal epithelial cells cultured on the amniotic membrane stromal matrix. Br J Ophthalmol 2001 Apr;85(4):444-449.

(12) Tseng SC, Li DQ, Ma X. Suppression of transforming growth factor-beta isoforms, TGF-beta receptor type II, and myofibroblast differentiation in cultured human corneal and limbal fibroblasts by amniotic membrane matrix. J Cell Physiol 1999 Jun;179(3):325-335.

(13) Mahmoudi-Rad M, Abolhasani E, Moravvej H, Mahmoudi-Rad N, Mirdamadi Y. Acellular amniotic membrane: an appropriate scaffold for fibroblast proliferation. Clin Exp Dermatol 2013 Aug;38(6):646-651.

(14) Yang L, Shirakata Y, Tokumaru S, Xiuju D, Tohyama M, Hanakawa Y, et al. Living skin equivalents constructed using human amnions as a matrix. J Dermatol Sci 2009 Dec;56(3):188-195.

(15) Teo AK, Vallier L. Emerging use of stem cells in regenerative medicine. Biochem J 2010 Apr 28;428(1):11-23.

(16) De Francesco F, Ricci G, D'Andrea F, Nicoletti GF, Ferraro GA. Human Adipose Stem Cells: From Bench to Bedside. Tissue Eng Part B Rev 2015 Dec;21(6):572-584.

(17) Ding DC, Chang YH, Shyu WC, Lin SZ. Human umbilical cord mesenchymal stem cells: a new era for stem cell therapy. Cell Transplant 2015;24(3):339-347.

(18) Lo B, Parham L. Ethical issues in stem cell research. Endocr Rev 2009 May;30(3):204-213.

(19) Riazi AM, Kwon SY, Stanford WL. Stem cell sources for regenerative medicine. Methods Mol Biol 2009;482:55-90.

(20) Zuk PA, Zhu M, Ashjian P, De Ugarte DA, Huang JI, Mizuno H, et al. Human adipose tissue is a source of multipotent stem cells. Mol Biol Cell 2002 Dec;13(12):4279-4295.

(21) Nae S, Bordeianu I, Stancioiu AT, Antohi N. Human adipose-derived stem cells: definition, isolation, tissue-engineering applications. Rom J Morphol Embryol 2013;54(4):919-924.

(22) Gao F, Chiu SM, Motan DA, Zhang Z, Chen L, Ji HL, et al. Mesenchymal stem cells and immunomodulation: current status and future prospects. Cell Death Dis 2016 Jan 21;7:e2062.

(23) Friedenstein AJ, Petrakova KV, Kurolesova AI, Frolova GP. Heterotopic of bone marrow. Analysis of precursor cells for osteogenic and hematopoietic tissues. Transplantation 1968 Mar;6(2):230-247.

(24) Lindroos B, Suuronen R, Miettinen S. The potential of adipose stem cells in regenerative medicine. Stem Cell Rev 2011 Jun;7(2):269-291.

(25) Strioga M, Viswanathan S, Darinskas A, Slaby O, Michalek J. Same or not the same? Comparison of adipose tissue-derived versus bone marrow-derived mesenchymal stem and stromal cells. Stem Cells Dev 2012 Sep 20;21(14):2724-2752.

(26) Toyserkani NM, Christensen ML, Sheikh SP, Sorensen JA. Adipose-Derived Stem Cells: New Treatment for Wound Healing? Ann Plast Surg 2015 Jul;75(1):117-123.

(27) Sasaki J, Hashimoto M, Yamaguchi S, Itoh Y, Yoshimoto I, Matsumoto T, et al. Fabrication of Biomimetic Bone Tissue Using Mesenchymal Stem Cell-Derived Three-Dimensional Constructs Incorporating Endothelial Cells. PLoS One 2015 Jun 5;10(6):e0129266.

(28) Pedersen TO, Blois AL, Xue Y, Xing Z, Sun Y, Finne-Wistrand A, et al. Mesenchymal stem cells induce endothelial cell quiescence and promote capillary formation. Stem Cell Res Ther 2014 Feb 17;5(1):23.

(29) Haase A, Olmer R, Schwanke K, Wunderlich S, Merkert S, Hess C, et al. Generation of induced pluripotent stem cells from human cord blood. Cell Stem Cell 2009 Oct 2;5(4):434-441.

(30) Sarkanen JR, Kaila V, Mannerstrom B, Raty S, Kuokkanen H, Miettinen S, et al. Human adipose tissue extract induces angiogenesis and adipogenesis in vitro. Tissue Eng Part A 2012 Jan;18(1-2):17-25.

(31) Sarkanen JR, Vuorenpaa H, Huttala O, Mannerstrom B, Kuokkanen H, Miettinen S, et al. Adipose stromal cell tubule network model provides a versatile tool for vascular research and tissue engineering. Cells Tissues Organs 2012;196(5):385-397.

(32) Nordback PH, Miettinen S, Kaariainen M, Pelto-Huikko M, Kuokkanen H, Suuronen R. Amniotic membrane reduces wound size in early stages of the healing process. J Wound Care 2012 Apr;21(4):190, 192-4, 196-7.

(33) Biosistemika LLC. qPCR Basics. Available at: http://biosistemika.com/workshops/qpcr-basics/. Accessed 10/29, 2016.

(34) Shan T, Liu W, Kuang S. Fatty acid binding protein 4 expression marks a population of adipocyte progenitors in white and brown adipose tissues. FASEB J 2013 Jan;27(1):277-287.

(35) Turner NA, Moake JL. Factor VIII Is Synthesized in Human Endothelial Cells, Packaged in Weibel-Palade Bodies and Secreted Bound to ULVWF Strings. PLoS One 2015 Oct 16;10(10):e0140740.

(36) Kedziorek DA, Kraitchman DL. Superparamagnetic iron oxide labeling of stem cells for MRI tracking and delivery in cardiovascular disease. Methods Mol Biol 2010;660:171-183.

(37) Guneta V, Tan NS, Chan SK, Tanavde V, Lim TC, Wong TC, et al. Comparative study of adipose-derived stem cells and bone marrow-derived stem cells in similar microenvironmental conditions. Exp Cell Res 2016 Nov 1;348(2):155-164.

(38) Lei J, Peng S, Samuel SB, Zhang S, Wu Y, Wang P, et al. A simple and biosafe method for isolation of human umbilical vein endothelial cells. Anal Biochem 2016 Sep 1;508:15-18.

(39) Hänninen ea. Manuscript in preparation.

(40) Rohaina CM, Then KY, Ng AM, Wan Abdul Halim WH, Zahidin AZ, Saim A, et al. Reconstruction of limbal stem cell deficient corneal surface with induced human bone marrow mesenchymal stem cells on amniotic membrane. Transl Res 2014 Mar;163(3):200-210.

(41) Ghazaryan E, Zhang Y, He Y, Liu X, Li Y, Xie J, et al. Mesenchymal stem cells in corneal neovascularization: Comparison of different application routes. Mol Med Rep 2016 Oct;14(4):3104-3112.

(42) Samadikuchaksaraei A, Mehdipour A, Habibi Roudkenar M, Verdi J, Joghataei MT, As'adi K, et al. A Dermal Equivalent Engineered with TGF-beta3 Expressing Bone Marrow Stromal Cells and Amniotic Membrane: Cosmetic Healing of Full-Thickness Skin Wounds in Rats. Artif Organs 2016 Dec;40(12):E266-E279.

(43) Roux S, Bodivit G, Bartis W, Lebouvier A, Chevallier N, Fialaire-Legendre A, et al. In Vitro Characterization of Patches of Human Mesenchymal Stromal Cells. Tissue Eng Part A 2015 Feb 1;21(3-4):417-425.

(44) Varga I, Miko M, Oravcova L, Backayova T, Koller J, Danisovic L. Ultra-structural morphology of long-term cultivated white adipose tissue-derived stem cells. Cell Tissue Bank 2015 Dec;16(4):639-647.

(45) Roxburgh J, Metcalfe AD, Martin YH. The effect of medium selection on adipose-derived stem cell expansion and differentiation: implications for application in regenerative medicine. Cytotechnology 2016 Aug;68(4):957-967.

(46) Kachgal S, Putnam AJ. Mesenchymal stem cells from adipose and bone marrow promote angiogenesis via distinct cytokine and protease expression mechanisms. Angiogenesis 2011 Mar;14(1):47-59.

(47) Jiang F, Ma J, Liang Y, Niu Y, Chen N, Shen M. Amniotic Mesenchymal Stem Cells Can Enhance Angiogenic Capacity via MMPs In Vitro and In Vivo. Biomed Res Int 2015;2015:324014.

(48) Merfeld-Clauss S, Gollahalli N, March KL, Traktuev DO. Adipose tissue progenitor cells directly interact with endothelial cells to induce vascular network formation. Tissue Eng Part A 2010 Sep;16(9):2953-2966.

(49) Matsuda K, Falkenberg KJ, Woods AA, Choi YS, Morrison WA, Dilley RJ. Adipose-Derived Stem Cells Promote Angiogenesis and Tissue Formation for In Vivo Tissue Engineering. Tissue Eng Part A 2013 Jun;19(11-12):1327-1335.

(50) Lin CC, Fu SJ. Osteogenesis of human adipose-derived stem cells on poly(dopamine)-coated electrospun poly(lactic acid) fiber mats. Mater Sci Eng C Mater Biol Appl 2016 Jan 1;58:254-263.

(51) Kingham PJ, Kolar MK, Novikova LN, Novikov LN, Wiberg M. Stimulating the neurotrophic and angiogenic properties of human adipose-derived stem cells enhances nerve repair. Stem Cells Dev 2014 Apr 1;23(7):741-754.

(52) Choi BH, Choi KH, Lee HS, Song BR, Park SR, Yang JW, et al. Inhibition of blood vessel formation by a chondrocyte-derived extracellular matrix. Biomaterials 2014 Jul;35(22):5711-5720.

(53) Chua WK, Oyen ML. Do we know the strength of the chorioamnion? A critical review and analysis. Eur J Obstet Gynecol Reprod Biol 2009 May;144 Suppl 1:S128-33.

(54) Oyen ML, Calvin SE, Cook RF. Uniaxial stress-relaxation and stress-strain responses of human amnion. J Mater Sci Mater Med 2004 May;15(5):619-624.

(55) Amensag S, McFetridge PS. Rolling the human amnion to engineer laminated vascular tissues. Tissue Eng Part C Methods 2012 Nov;18(11):903-912.

(56) Chua WK, Oyen ML. Do we know the strength of the chorioamnion? A critical review and analysis. Eur J Obstet Gynecol Reprod Biol 2009 May;144 Suppl 1:S128-33.

(57) Cross section of the human Amniotic Membrane. Available at: https://nextbio.co.za/amniomatrix-2-2/. Accessed 10/27, 2016.

(58) Hierarchy of stem cells. Available at: http://oerpub.github.io/epubjs-demo-book/content/m46036.xhtml. Accessed 10/29, 2016.